

AN INVESTIGATION OF TRANSGRESSIVE BARRIERS IN
LATE PLEISTOCENE LAKE BONNEVILLE

by

Katherine Hart Schide

A thesis submitted to the faculty of
The University of Utah
in partial fulfillment of the requirements for the degree of

Master of Science

in

Geology

Department of Geology and Geophysics

The University of Utah

August 2016

Copyright © Katherine Hart Schide 2016

All Rights Reserved

The University of Utah Graduate School

STATEMENT OF THESIS APPROVAL

The thesis of **Katherine Hart Schide**
has been approved by the following supervisory committee members:

<u>Paul Jewell</u>	, Chair	<u>5/12/2016</u> Date Approved
<u>Jeffrey Moore</u>	, Member	<u>5/12/2016</u> Date Approved
<u>Charles Oviatt</u>	, Member	<u>5/12/2016</u> Date Approved

and by **John Bartley**, Chair of
the Department of **Geology and Geophysics**

and by David B. Kieda, Dean of The Graduate School.

ABSTRACT

Lake Bonneville was the largest of the Pleistocene pluvial lakes that once filled part of the Great Basin of the interior western United States. As the lake reached its highest level at the Bonneville shoreline and overflowed, it eroded through alluvium at Red Rock Pass, Idaho, and quickly dropped over 100 m to the Provo shoreline. This unique flooding history and resulting rapid lake-level fall allows us to assume that all other shorelines with elevations between the Bonneville and Provo levels formed during the lake's transgressive phase. Various types of depositional features characterize the shorelines within this transgressive interval, including many forms of barriers. This study uses 5-m auto-correlated digital elevation models (DEMs), airborne light detection and ranging (lidar), and ground-penetrating radar (GPR) surveys to measure the internal and external structure of intermediate barriers in late Pleistocene Lake Bonneville. Corrections for differential isostatic rebound reveal only one confidently correlatable intermediate shoreline at 1530 m (± 4 m) while differences in barrier morphology indicate that the formation of depositional features is highly dependent on local, not basin-scale, conditions.

TABLE OF CONTENTS

ABSTRACT.....	iii
LIST OF FIGURES	vi
ACKNOWLEDGEMENTS	viii
INTRODUCTION	1
Previous Work	4
Barriers.....	5
Purpose.....	6
METHODS	8
Field Locations.....	8
Data Sources	8
Elevation Selection Methodology.....	14
Isostatic Corrections.....	15
Statistical Significance.....	16
Ground-Penetrating Radar	17
RESULTS	20
Distribution and Characteristics of Barriers	20
Bonneville and Provo Shorelines.....	24
Ground-Penetrating Radar	24
Quantitative Analysis.....	27
DISCUSSION	30
Controls on Barrier Bar Formation	30
Interpreting the Subsurface	34
Significance of Barrier Elevations and Comparison to Erosional Shorelines	34
Paleoclimate Implications.....	36
CONCLUSIONS.....	38

APPENDICES

A: DETAILED RESULTS OF GROUND-PENETRATING RADAR	40
B: QUANTITATIVE ANALYSES	50
REFERENCES	53

LIST OF FIGURES

1. Area map of the maximum extent of Late Pleistocene Lake Bonneville	2
2. A Lake Bonneville hydrograph.....	3
3. Profiles of barriers at Monument Valley and Matlin 1	13
4. GPR profiles at Matlin 1	18
5. GPR profiles at Horse Hills 2	19
6. Box plots showing physical propperties of intermediate barriers.....	21
7. Examples of barrier classifications	22
8. Images and profiles of barriers at Dugway 1 and 2	23
9. A stream drainage proves suitable conditions for the formation of barriers.....	25
10. A scatterplot of measured Bonneville and upper Provo shoreline elevations..	26
11. PDF plots evaluated with a 4-m moving window every 0.5 m.....	28
12.The relationship between changes in water level and sediment supply.....	31
13. GPR survey at Matlin 1 on the Bonneville-level barrier	41
14. GPR survey at Matlin 1 on the Bonneville-level barrier	42
15. A common midpoint sounding at Matlin 1	43
16. GPR survey at Matlin 1 on an intermediate-level barrier	44
17. GPR survey at Matlin 1 on an intermediate-level barrier	45
18. A common midpoint sounding at Matlin 1	46
19. GPR survey at Horse Hills 2 on the Bonneville-level barrier.....	47

20. GPR survey at Horse Hills 2 on the Bonneville-level barrier.....	48
21. A common midpoint sounding at Horse Hills 2	49
22. PDF plot of barrier and random sample elevations	51
23. PDF plot of erosional shorelines and random sample elevations	52

ACKNOWLEDGEMENTS

I would like to thank my advisor, Paul Jewell, for his continued support and insight over the last 2 years. Thank you for long days in the desert, many flat tire changes, and my last-minute route to graduate school.

Thank you to Jack Oviatt for providing endless knowledge of the Bonneville Basin and guidance through the duration of this project, as well as to Harry Jol and his students, who led all GPR campaigns with unmatched energy. I would also like to acknowledge my committee member Jeff Moore for offering sound advice in my decision to continue in this field.

Simon Brewer was instrumental in guiding the statistical analyses and I thank him for going out of his way to help me with this project. Thanks to Daren Nelson for sharing data, ideas, and a day in the desert.

To my friends in the Department of Geology and Geophysics, thank you for rock garden lunches, midmorning coffee breaks, and continuing to keep me excited about earth science.

Lastly, I would like to thank my parents who took me outside, answered my questions, and made this education possible.

INTRODUCTION

Landscapes act as continuous recorders of changing climate. Investigating the ways in which rivers, lakes, and ice interact with Earth's surface provides a better understanding of past climate and its relationship with the landscape. In the west desert of Utah, shorelines and lacustrine features in barren valleys reveal a time when precipitation outmatched evaporation (Benson et al., 1990; Godsey, Currey, & Chan, 2005; Oviatt, 1997). This area of the internally drained Great Basin once supported Lake Bonneville, the largest of the Quaternary pluvial lakes in the western United States (Figure 1).

First studied in detail by Gilbert (1890), Lake Bonneville has received significant attention over the past century due to its size, unique history, and well-preserved shorelines. Extensive studies (Currey, 1990; Oviatt, 1997; Oviatt, 2015; Oviatt, Currey, & Sack, 1992) outline the lake's oscillatory transgression to its highstand at the Bonneville shoreline, where it eroded through alluvial, landslide, and Neogene deposits at Red Rock Pass, Idaho, causing the lake to catastrophically flood north into the Snake River drainage and quickly drop over 100 m to the Provo shoreline where it stabilized and remained for nearly 3,000 years (Godsey et al., 2005; Godsey, Oviatt, Miller, & Chan, 2011; Oviatt, 2015; Figure 2).

In addition to these named shorelines, hundreds of other lacustrine features are found at intermediate elevations below the Bonneville shoreline and above the well-developed Provo shoreline. Due to the nearly instantaneous drop in water level during the

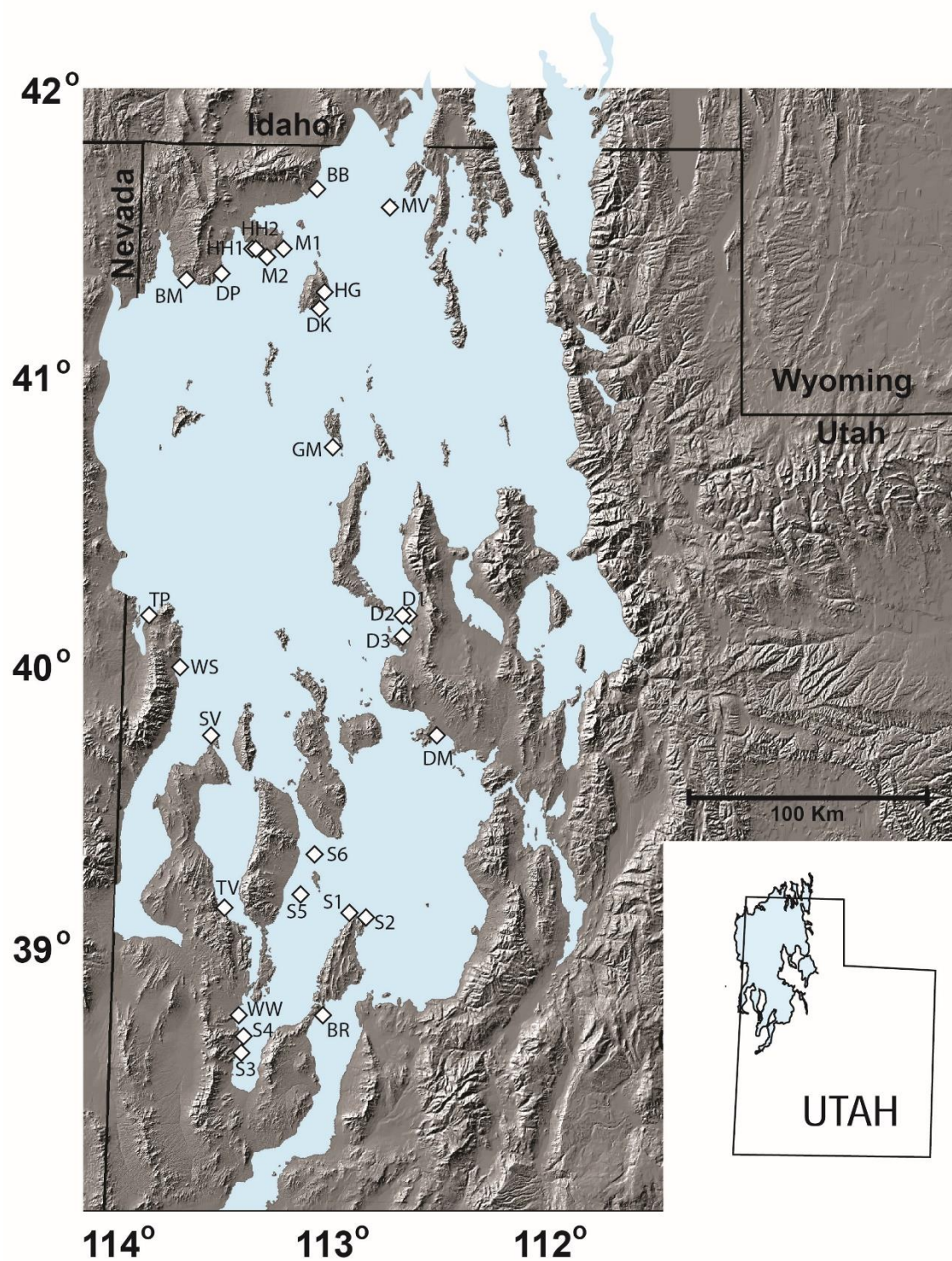


Figure 1. Area map of the maximum extent of Late Pleistocene Lake Bonneville. After Jewell (2016). See Table 1 for location abbreviations.

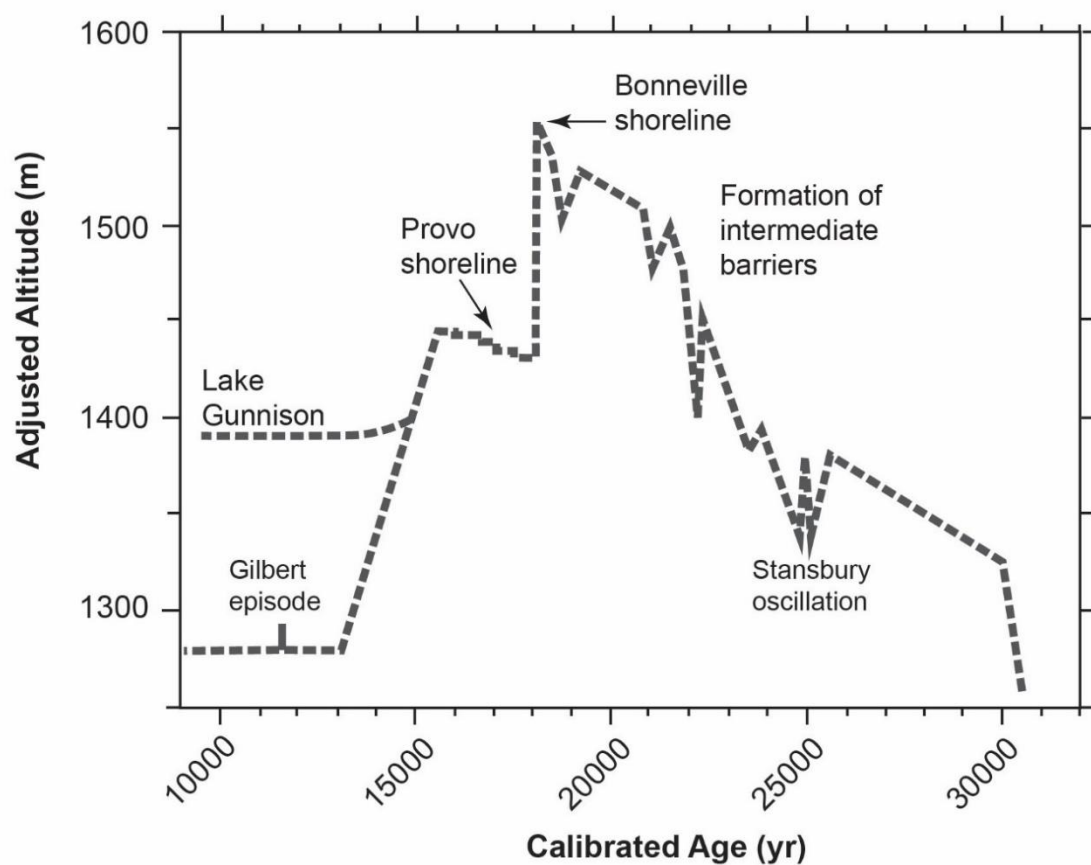


Figure 2. A Lake Bonneville hydrograph. After Oviatt (2015).

Bonneville flood, these features had to be formed during the transgressive phase, as the lake filled with water during the late Pleistocene.

Previous Work

Gilbert (1890) referred to sea cliffs, cut terraces, and constructional features found between the Bonneville and Provo shorelines as “Intermediate shorelines and embankments”. Gilbert outlined cross-sectional profiles of the intermediate shorelines at 10 locations and attempted to correlate their elevations on both local and basin scales. One horizon 4.5 – 7.5 m below the Bonneville shoreline is noticeable in eight of the localities he investigated, but otherwise, Gilbert concluded that “...there are no correspondences which can not be referred to fortuitous coincidence” (p. 139). To explain the lack of correlation between intermediate shorelines, Gilbert (1890) proposed the “Hypothesis of Oscillating Water Surface” (p. 141). According to this hypothesis, the vertical interval between constructional embankments is a function of such factors as local wave magnitude, the direction of incoming wave trains relative to the local shore configuration, sediment supply, slope, and possibly other geomorphic factors. As the lake levels rose and fell, the slope of the shoreface determined the local water depth and thus the rate of growth of depositional features. For example, a relatively small change in lake level could lead to aggradation of an existing embankment in one place while resulting in a complete overstep in another. Gilbert (1890) explained that the intermediate embankments record the effects of an oscillating water surface based on the individual morphology of each shoreface.

More recent studies of modern and paleo lake systems further confirmed Gilbert’s

theories. Atwood (1994) surveyed shorelines on Antelope Island in the Great Salt Lake, the modern lake that now resides in the Lake Bonneville basin near Salt Lake City, Utah. Measurements of the debris line from the 1980s highstand revealed shoreline elevations up to nearly 2 m above the highest still-water level. Atwood (1994) attributed these differences to local lake bed geometry and varying exposure to storm waves, as the higher shorelines were found where fetch is greatest. In addition, a paleo-shoreline study in the Jessup embayment of late Pleistocene Lake Lahontan found up to 2.6 m of variation in the elevation of constructional shorelines (Adams & Wesnousky, 1998). This study also explored the timescales of still-stand recorded by such features, describing the relatively rapid formation of barriers in modern Pyramid Lake that took place over 7 months in 1997 (Adams & Wesnousky, 1998). Previous work since Gilbert's (1890) investigation of closed-basin, lacustrine shorelines clearly demonstrates the local variability of these features and the short timescales over which they can be built.

In a recent study of Lake Bonneville shorelines, Jewell (2016) revisited Gilbert's (1890) attempt at correlating intermediate levels basin-wide. Using high-resolution digital elevation models (DEMs), the study documented five distinct levels based on elevations of erosional cut terraces at various locations throughout the basin. This was the first successful attempt at correlating intermediate shorelines in late Pleistocene Lake Bonneville.

Barriers

Barriers are elongated, coastal landforms that extend parallel to the shoreline, often across the mouths of inlets or embayments. They are composed of sand and/or

gravel transported by waves and currents and differ from marine bars in that they stand above the level of the highest tides. In the simplest terms, a barrier acts as a division between the main water body and the shore. There are several types of barriers with varying degrees of connectedness to the mainland; these include barrier islands, bayhead barriers, baymouth barriers, and barrier spits. Given the inconsistent nomenclature in the coastal geomorphology literature, this study adheres to the above definition of barriers (Bird, 2008; Gilbert, 1885; Hesp & Short, 1999; Leatherman, 1988; Masselink & Hughs, 2003; Woodroffe, 2003).

Since Gilbert (1885) first identified and described barriers in the Lake Bonneville basin, there has been debate over a standard model for barrier formation (Davis, 1994a; review in Hesp & Short, 1999). Most agree that barriers form through some type of landward transport and upward accretion of coarse sediment (sand and/or gravel) (Davis, 1994a), the details of which depend on local conditions (Gilbert, 1885; Hesp & Short, 1999; Woodroffe, 2003). Despite their widespread prevalence in coastal environments, the processes that determine the size, shape, and position of barriers are not well defined or understood.

Purpose

This study expands on the work of Jewell (2016) and describes the observations and interpretations of barriers that formed during the lake's transgressive phase. Erosional cut terraces are assumed to be more reliable recorders of persistent water levels as they are less affected by localized sediment availability and secondary erosion (Gilbert, 1890). However, this investigation of depositional features explores Gilbert's

(1885, 1890) hypothesis that local conditions affecting wave magnitude, rather than basin-wide water level changes, exert primary control on the presence and morphology of the intermediate embankments. This study uses ground-penetrating radar (GPR), high-resolution DEMs, and field observations to analyze the morphology, elevation, and location of barriers in late Pleistocene Lake Bonneville.

METHODS

Field Locations

This study analyzed 102 intermediate-level barriers at 26 locations across the Bonneville Basin (Figure 1, Table 1). A lidar survey acquired in this study provided 0.5-m and 0.3-m DEMs for Matlin 1 and Monument Valley while all other locations were studied using 5-m DEMs (Figure 3). We visited Black Butte, Matlin 1 and 2, Horse Hills 1 and 2, Devil's Playground, Bovine Mountains, Grassy Mountains, and Dugway 1, 2, and 3 during field campaigns in the spring and fall of 2015.

Data Sources

The majority of data used in this study were derived from maps made from publicly available bare-earth DEMs generated by the State of Utah (<http://gis.utah.gov/data>). In a few locations, additional light detection and ranging (lidar) surveys flown by researchers at the University of Alaska provide higher resolution terrain data (Figure 3). The DEMs produced from lidar data have 0.5-m or 0.3-m horizontal and 0.2-m vertical resolution. The publically available 5-m auto-correlated DEMs were created using imagery from the 2006 NAIP survey and have 4-m vertical resolution. However, in places where lidar and 5-m DEMs are both available, the vertical resolution of the 5-m data appears to be better than reported (Figure 3). This provides additional confidence in the accuracy of barrier elevations measured from the 5-m DEMs, but

Table 1. Classifications and measurements of all barriers analyzed in this study. UTM coordinates in reference to zone 12N. BHB = Bayhead barrier, BS = Barrier spit, BI = Barrier island. B = Bonneville, P = Provo, I = Intermediate.

	Location	Shore-line	Measured Elevation	Corrected Elevation	Classification	Length (m)	Width (m)	Area (m ²)
BB	<i>Black Butte</i> <i>317764 4634013</i>	B	1582	1552				
		I	1561	1532	BHB	1953	120	189275
		I	1545	1517	BHB	1923	155	189899
		I	1530	1502	BHB	1480	148	174436
		I	1513	1486	BHB	735	115	64657
		P	1470	1445				
BR	<i>Black Rock Pass</i> <i>321452 4286276</i>	B	1564	1552				
		I	1548	1540	BHB	436	117	47936
		I	1539	1531	BHB	661	103	45798
		I	1541	1529	BHB	301	141	39842
		I	1531	1520	BHB	628	181	77584
		I	1524	1513	BS	633	141	82867
		I	1503	1493	BS	846	142	108343
BM	<i>Bovine Mountains</i> <i>265934 4593689</i>	B	1588	1552				
		I	1560	1525	BS	1158	143	120101
		I	1520	1488	BS	1579	153	121999
		I	1506	1474	BS	1962	164	218892
		P	1475	1445				
DK	<i>Deadmans Knoll</i> <i>321157 4583504</i>	B	1613	1552				
		I	1589	1530	BHB	481	241	103295
		I	1568	1511	BHB	947	231	178588
		I	1542	1488	BHB	981	116	115895
		P	1495	1445				
DM	<i>Desert Mountains</i> <i>371036 4403206</i>	B	1580	1552				
		I	1554	1528	BS	3906	533	2E+06
		I	1536	1512	BS	5144	445	2E+06
		P	1462	1445				
DP	<i>Devils Playground</i> <i>279284 4597824</i>	B	1590	1552				
		I	1574	1538	BHB	348	63	21155
		I	1566	1531	BHB	562	140	71126
		I	1552	1518	BHB	711	160	138784
		I	1535	1503	BHB	860	124	94659
		I	1522	1491	BHB	795	161	119844
		P	1470	1445				
D1	<i>Dugway 1</i> <i>358671 4452890</i>	B	1597	1552				
		I	1583	1539	BHB	1910	172	297475
		I	1565	1523	BHB	2487	260	505367
		I	1543	1503	BS	2493	183	343754
		I	1530	1491	BS	2235	224	459711
		P	1480	1445				
D2	<i>Dugway 2</i> <i>355939 4452002</i>	B	1597	1552				
		I	1515	1476	BHB	908	232	207213
		I	1499	1462	BS	958	109	93237
		I	1500	1463	BHB	1719	186	279602
		P	1481	1445				

Table 1. Continued

Location	Shore-line	Measured Elevation	Corrected Elevation	Classification	Length (m)	Width (m)	Area (m ²)
D3 <i>Dugway 3</i> 357464 4443951	B	1596	1552				
	I	1580	1537	BHB	1300	268	225302
	I	1572	1530	BHB	1612	269	460276
	I	1558	1517	BHB	1400	188	252376
	P	1481	1445				
M1 <i>Matlin 1</i> 305477 4608736	B	1596	1552				
	I	1572	1530	BHB	2022	184	306993
	I	1551	1510	BHB	1507	203	296305
	I	1529	1490	BHB	1544	192	211199
	I	1510	1472	BS	2086	143	146371
	I	1492	1455	BS	2100	90	186472
M2 <i>Matlin 2</i> 301487 4608736	B	1594	1552				
	I	1581	1540	BS	845	120	61523
	I	1570	1529	BS	677	94	46507
	P	1482	1445				
GM <i>Grassy Mountains</i> 328439 4528972	B	1623	1552				
	I	1600	1533	BHB	1335	195	279514
	I	1577	1514	BHB	1257	191	255993
	I	1556	1496	BHB	752	169	132029
PG <i>Hogup</i> 322801 4589969	B	1612	1552				
	I	1585	1527	BHB	841	129	90141
	I	1563	1507	BHB	895	132	86165
	I	1543	1489	BHB	730	112	93510
	P	1495	1445				
HH1 <i>Horse Hills 1</i> 294727 4610517	B	1591	1552				
	I	1560	1523	BHB	844	92	73476
	I	1534	1499	BHB	1266	162	220867
	P	1477	1445				
HH2 <i>Horse Hills 2</i> 296889 4610122	B	1590	1552				
	I	1563	1526	BHB	836	50	38659
	I	1552	1516	BHB	772	40	25047
	I	1535	1500	BHB	721	131	96693
MV <i>Monument Valley</i> 349672 4626122	B	1592	1552				
	I	1535	1500	BHB	740	133	105562
	I	1512	1479	BHB	940	139	103733
	I	1496	1464	BHB	753	88	58794
	I	1533	1498	BHB	728	310	210565
P <i>Sevier 1</i> 337103 4326604	B	1475	1445				
	I	1573	1552				
	I	1563	1542	BHB	249	94	30073
	I	1555	1535	BHB	221	114	71060
	I	1526	1507	BS	757	87	24630
P <i>Sevier 1</i> 337103 4326604	I	1462	1445				
	P	1462	1445				

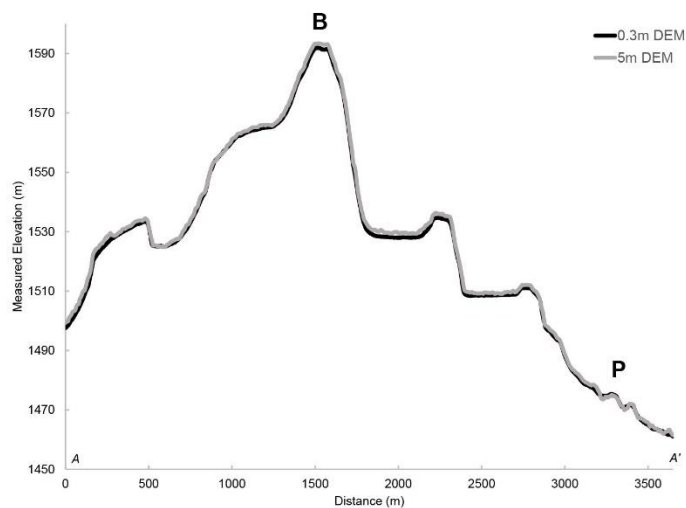
Table 1. Continued

	Location	Shore- line	Measured Elevation	Corrected Elevation	Classific- ation	Length (m)	Width (m)	Area (m ²)
S2	<i>Sevier 2</i> 339836 4326420	B	1574	1552				
		I	1563	1542	BHB	413	80	46772
		I	1547	1527	BHB	439	101	39797
		I	1530	1511	BHB	529	88	42741
		I	1518	1499	BHB	494	97	60277
		I	1504	1486	BHB	457	140	45106
		P	1460	1445				
S3	<i>Sevier 3</i> 288463 4270991	B	1560	1552				
		I	1536	1526	BI	1266	192	172222
		I	1522	1511	BI	1300	126	141184
		I	1505	1493	BI	1460	186	170174
		I	1480	1466	BI	2686	224	591998
		P	1461	1445				
S4	<i>Sevier 4</i> 289423 4276575	B	1560	1552				
		I	1514	1502	BS	265	124	30823
		I	1508	1496	BS	597	66	67497
		I	1492	1479	BS	495	130	34007
		I	1482	1468	BS	596	150	84612
		P	1461	1445				
S5	<i>Sevier 5</i> 314002 4337957	B	1576	1552				
		I	1520	1499	BHB	2389	216	464354
		I	1508	1488	BHB	2361	253	505041
		I	1501	1481	BHB	2255	175	410753
		I	1492	1472	BHB	3450	223	822862
		I	1481	1462	BHB	3612	275	992184
		P	1463	1445				
S6	<i>Sevier 6</i> 320171 4351536	B	1576	1552				
		I	1514	1493	BHB	414	102	31217
		I	1506	1486	BHB	904	140	75632
		I	1501	1481	BHB	778	120	64185
		I	1498	1478	BHB	682	118	135353
		I	1495	1475	BHB	1565	123	281967
		I	1493	1473	BHB	1655	166	117036
		I	1488	1469	BHB	1082	124	124712
		P	1463	1445				
SV	<i>Snake Valley</i> 274270 4401720	B	1583	1552				
		I	1526	1499	BHB	1041	260	238855
		I	1512	1487	BHB	884	69	69178
		I	1506	1481	BHB	690	112	81724
		I	1495	1471	BHB	1068	74	76212
		P	1467	1445				
TV	<i>Tule Valley</i> 281587 4330484	B	1565	1552				
		I	1545	1532	BHB	680	113	74494
		I	1507	1495	BHB	862	134	118754
		I	1489	1477	BHB	517	107	46592
		P	1456	1445				
TP	<i>Twin Peaks</i> 247815 4456591	B	1590	1552				
		I	1567	1530	BHB	1253	188	233837
		I	1552	1515	BHB	1340	165	220952
		I	1539	1502	BHB	809	159	117892
		P	1480	1445				

Table 1. Continued

Location		Shore- line	Measured Elevation	Corrected Elevation	Classific- ation	Length (m)	Width (m)	Area (m ²)
WW	<i>WahWah</i> <i>287799 4285458</i>	B	1563	1552				
		I	1551	1539	BHB	281	83	20815
		I	1546	1534	BHB	342	86	25994
		I	1542	1530	BHB	530	97	44496
		I	1538	1526	BHB	790	80	45114
		P	1462	1445				
WS	<i>Willow Spring</i> <i>264203 4430879</i>	B	1589	1552				
		I	1579	1543	BI	617	187	84033
		I	1574	1538	BI	1259	207	118788
		I	1548	1514	BI	1045	172	137097
		I	1508	1477	BHB	800	79	62494
		I	1495	1465	BHB	1382	120	96419
		P	1474	1445				

Monument Valley



Matlin 1

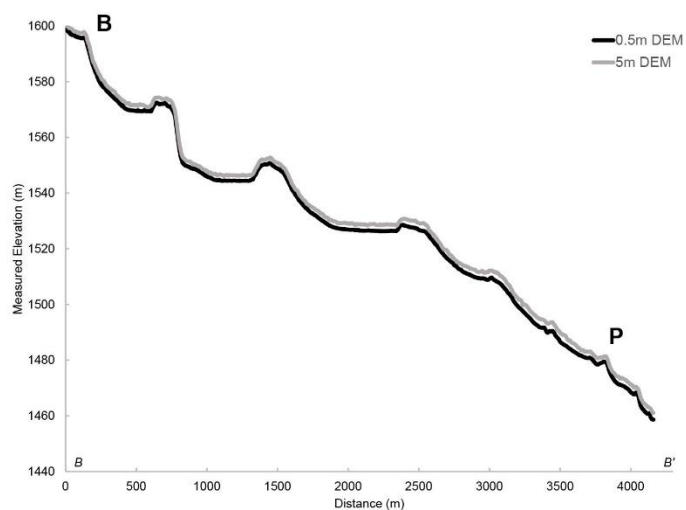


Figure 3. Profiles of barriers at Monument Valley and Matlin 1. DEMs produced by airborne lidar (0.3m and 0.5m) and auto-correlated aerial imagery (5m) do not show significant differences in their vertical measurements. B = Bonneville shoreline, P = Provo shoreline.

because this could only be tested in two locations, we still assume 4-m resolution.

Elevation Selection Methodology

We selected the barriers analyzed in this study from a basin-wide survey of depositional features based on the following:

- (1) Meet the criteria to be classified as barriers using the definition outlined above.
- (2) Local and identifiable Bonneville and Provo shorelines. The barriers must be at elevations between these two levels to ensure that they are transgressive features. Also, the Bonneville and Provo shorelines provide constraints for isostatic rebound corrections and thus must be measurable near the barriers.
- (3) Available 5-m DEMs or higher-resolution maps of the field site. This requirement eliminated all potential locations outside of the state of Utah where 5-m DEMs are not publically available.

We measured the elevations of each barrier on the highest resolution map available for that locality. Elevations were recorded as the highest point on a cross-section measured near the center of the feature. In some cases, the Bonneville and/or Provo levels were not expressed as barriers and thus had to be measured from other nearby shoreline features like embankments or beach ridges.

We measured the lengths, widths, and surface areas of the barriers in order to find general characteristics of the features. Lengths were measured along the crests of barriers from the point of connection to the mainland, to the opposite end – either to where the barriers reconnected to the mainland or to the end of the barrier spit. Widths were measured in locations that appeared representative of the entire barrier, between points of

elevation inflection with the underlying shorezone. Surface areas were determined by tracing the outlines of each barrier.

Isostatic Corrections

Isostatic rebound due to unloading from the time of the lake's highstand complicates attempts to correlate intermediate shorelines. For example, the elevation of the Bonneville shoreline varies up to 74 m across the basin, ranging from 1552 m, its assumed unrebounded elevation, to a maximum of 1626 m (Currey, 1982). A relationship proposed by Currey (in Currey & Oviatt, 1985; Oviatt et al., 1992) corrects measured shoreline elevations for isostatic rebound based on the local elevation of the Bonneville shoreline.

$$Z_a = Z_r - [(Z_r - 1200) / (Z_b - 1200)] * [Z_b - 1552] \quad (1)$$

Here, Z_a is the corrected elevation, while Z_r is the current measured elevation and Z_b is the local, measured Bonneville shoreline elevation. The lowest elevation in the basin is approximately 1200 m and 1552 m is the assumed elevation of the unrebounded Bonneville shoreline (Currey, 1982). Jewell (2016) modified this equation to

$$Z_a = Z_r - Z_b + 1552 \quad (2)$$

in order to only consider the elevation range between the Bonneville and Provo levels.

These corrected elevations are then normalized to fit a Bonneville-Provo vertical separation of 107 m, an arbitrary but reasonable value for rebound in the basin, which in this study range from 99 m to 128 m. The latter method works to identify relative shoreline elevations, using measured Provo and Bonneville shorelines to constrain the elevations at intermediate levels. This study uses the same methods as Jewell (2016) so

that shoreline and barrier elevations can be compared relative to the same datum.

Statistical Significance

In order to understand the significance of measured barrier elevations, the data were compared to a random sample of elevations between the Bonneville and Provo levels. Isostatically corrected outlines of the Bonneville and Provo shorelines (Daren Nelson, personal communication, unpublished work) were used to extract all intermediate elevation data from a basin-scale 30-m DEM in order to establish a random sample of elevation values. The probability density function (PDF) of corrected barrier elevations can then be compared to the PDF of this random sample to determine the likelihood that the measured distribution of elevations is different from the comparison sample. Significance of identified peaks was determined using the 95% confidence interval assuming a normal distribution using the following method:

$$p_i = \frac{c_i}{n} \quad (3)$$

$$95\% \text{ confidence interval} = p_i \pm 1.96 \sqrt{\frac{p_i(1-p_i)}{n}} \quad (4)$$

where c_i is the count of elevations in each bin, n is the total number of measured elevations, p_i is the probability, and 1.96 is the standard deviation of the mean that includes 95% of the area of a normal distribution. If the confidence interval (Equation 4) on the PDF of measured barrier elevations overlaps the PDF of the random sample, then the measured elevation is not different from the random sample. However, if the confidence interval does not overlap the PDF of the random data set, then there is a 95% probability that the difference is not due to chance and is considered significant (Cressie & Wikle, 2011).

Ground-Penetrating Radar

GPR is a noninvasive, geophysical method that identifies sedimentary boundaries in the subsurface using electromagnetic waves. These waves are projected downward into the ground and their two-way travel times are affected by changes in impedance that are then interpreted to represent changes in lithology. By determining the transmission velocity of the waves, the measured travel times can be converted to equivalent depths. The collection methods used in this study follow those of Jol and Bristow (2003) and the surveys were led by researchers from the University of Wisconsin - Eau Claire.

During a field campaign in June, 2015, four GPR profiles were collected on two barriers at Matlin 1 and two profiles were collected on the Bonneville level barrier at Horse Hills (Figure 4, Figure 5). An unshielded Sensors and Software® pulseEKKO GPR system with 100 MHz antennae, 1-m separation, and 0.5-m step size was used for all profiles. A common mid-point profile (CMP) was also collected in both locations in order to model the velocity and the dielectric properties of the sediments (Appendix A).

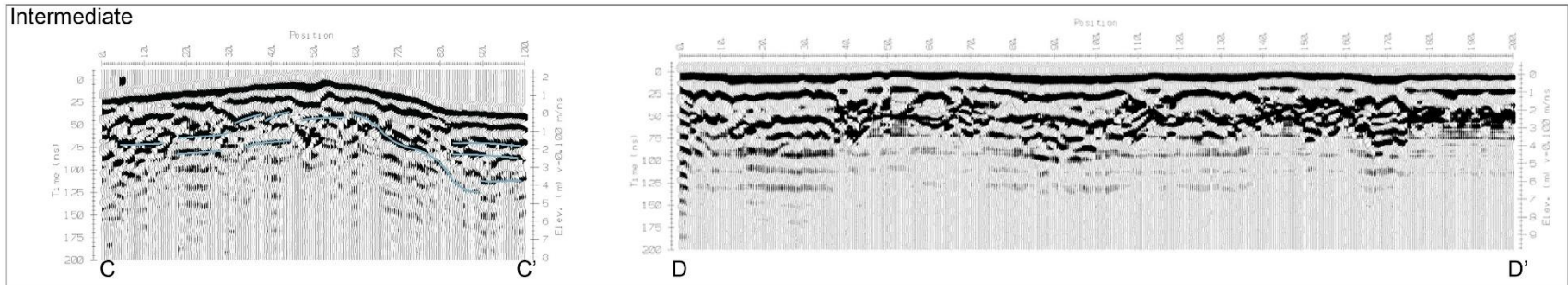
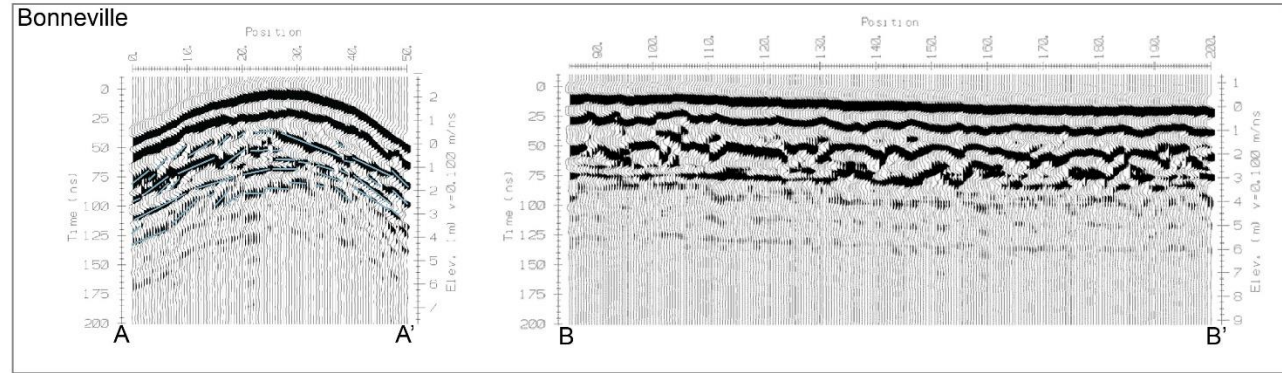


Figure 4. GPR profiles at Matlin 1. Surveys in this locality show the first 3-5 m of subsurface stratigraphy. Both the two-way travel times and converted depths are shown on the vertical axis. Position on the horizontal axis is given in meters. The dark bands represent changes in sedimentary properties as indicated by the travel times of waves recorded at the surface.

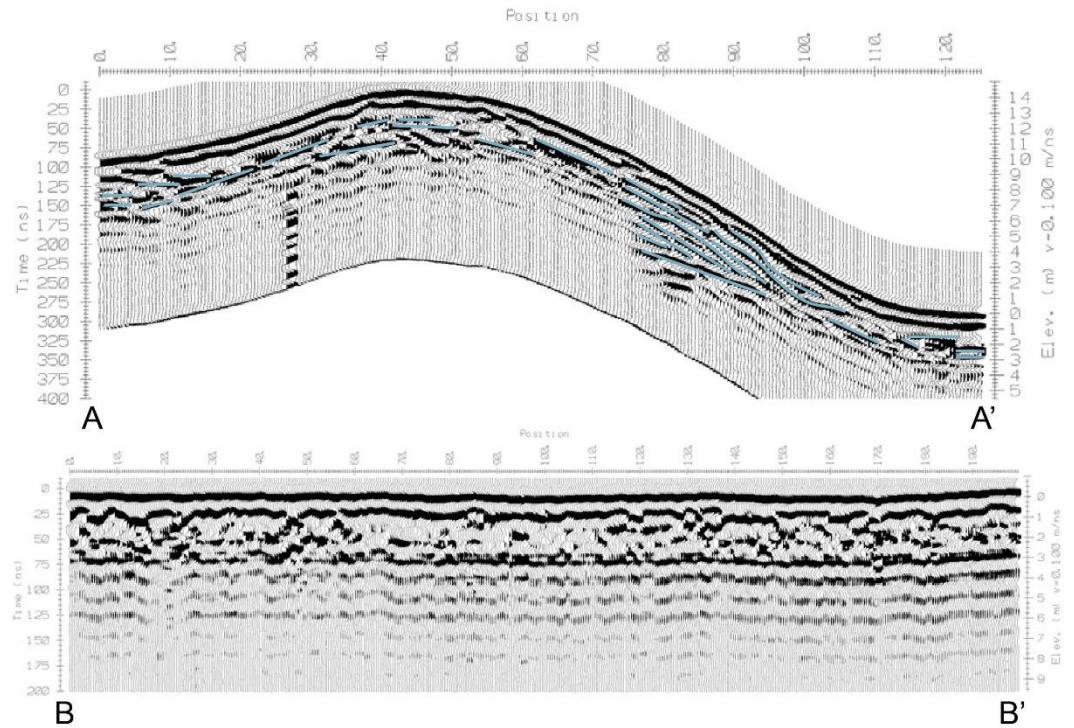
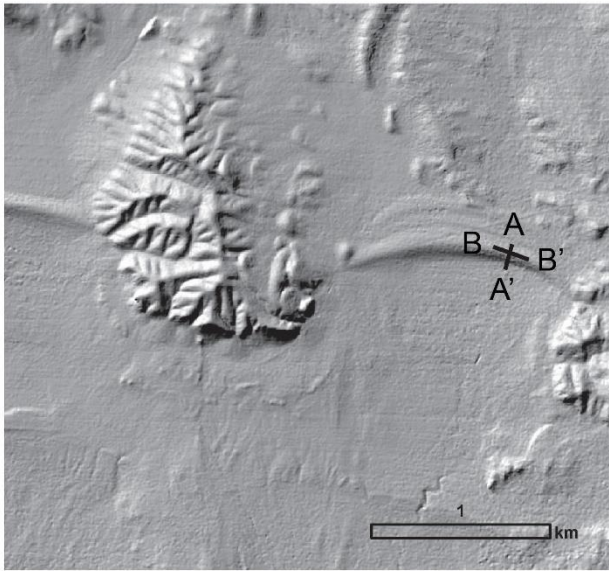


Figure 5. GPR profiles at Horse Hills 2. A survey of the Bonneville-level barrier reveals as much as the first 6 m of the subsurface.

RESULTS

Distribution and Characteristics of Barriers

The barriers identified in this study are primarily found on the northern and southwestern shorelines of the lake (Figure 1). The lack of barriers on the eastern side of the basin could in part be attributed to modern development, infrastructure, and gravel mining along the Wasatch Front. However, other factors like wind direction, shore zone slope angle, and secondary erosion processes may contribute to this spatial distribution.

Barriers appear in sets of up to seven throughout the Bonneville basin, typically in protected or enclosed terrain but with varying shapes and sizes. Barriers range from ~200 m to ~5 km in length and ~40 m to ~500 m in width, but the majority are less than 2.5 km long and 275 m wide. The median surface area of all barriers is ~112,000 m², with measurements ranging between ~21,000 m² and ~1.9*10⁶ m² (Figure 6). Of all measured features, 76 are classified as bayhead barriers, connecting to a bedrock outcrop and/or alluvial or colluvial fans on both sides. However, 19 only connect to the mainland on one side and are thus called barrier spits, while seven have no connection and are categorized as barrier islands (Figure 7). The shorter bayhead barriers are typically wider and more symmetrical than those that span larger embayments or are classified as barrier spits. In some locations, a clear direction of longshore drift is indicated by shorelines excavated from fan deposits that gradually change to barrier-deposit shorelines in the direction of transport (Figure 8). In other locations, barriers cross incised stream drainages, which

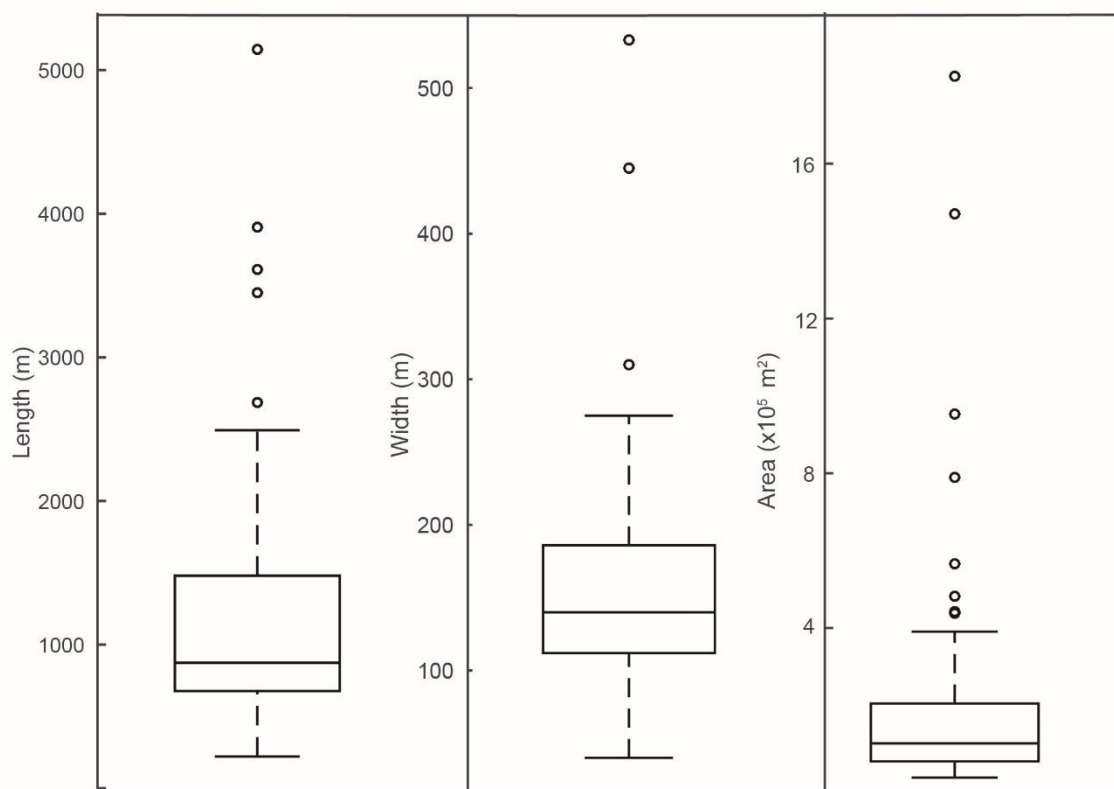


Figure 6. Box plots showing the physical properties of intermediate barriers. The box represents the middle 50% of the data with the whiskers encompassing the upper and lower 25%. Circles represent outliers. These features are found in a wide range of shapes and sizes and are not normally distributed. Three or more outliers exist in each of these measurement parameters, making it difficult to determine expected values of barrier morphology ($n = 102$).

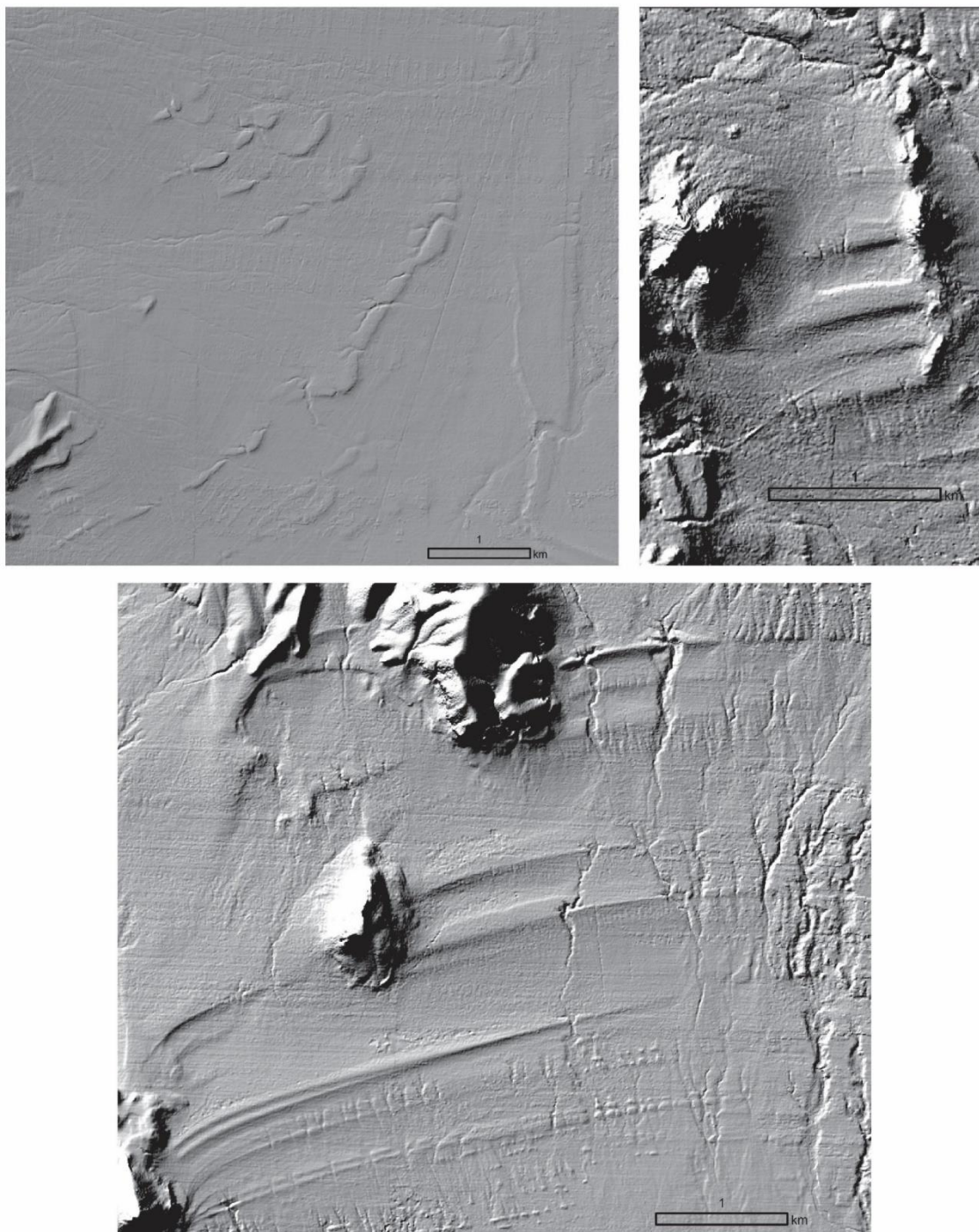


Figure 7. Examples of barrier classifications. A. Barrier islands at Sevier 8 (S8) B. Bayhead barriers at Devils Playground (DP) C. Barrier spits at Bovine Mountains (BM). See Table 1.

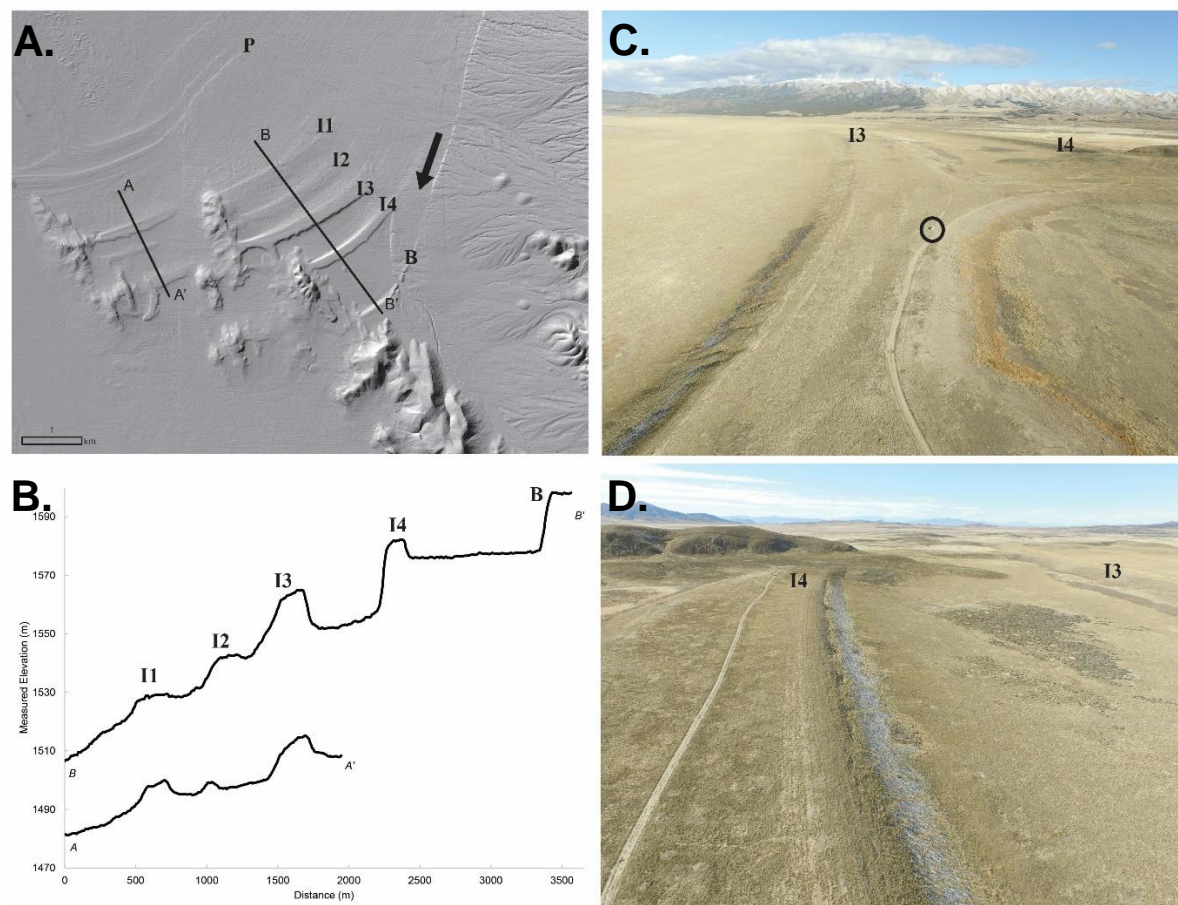


Figure 8. Images and profiles of barriers at Dugway 1 and 2 (Table 1). These barriers are constructed by sediments excavated from an alluvial fan and transported through longshore drift. A. 5-m DEM with measured cross-sections, labeled intermediate barriers, and arrow indicating direction of transport. B. Cross-sectional profiles of the eastern and western barriers reveal very different elevations despite their linear orientation. C. Photo taken from an unmanned aerial vehicle (UAV) looking east over I3. Truck is circled for scale. D. UAV photo looking west over I4.

provide a continuous sediment supply in a small bay necessary for construction and preservation (Figure 9).

Bonneville and Provo Shorelines

Elevations of the Bonneville and Provo shorelines measured in this study show vertical separations of 99 to 128 m, a slightly larger range than that identified by Jewell (2016) and Miller, Oviatt, and Mcgeehin (2013). With this greater total vertical separation comes a slightly weaker correlation between the two shoreline elevations (Figure 10). The DEMs used in this study have greater variability than the 1-m and 0.5-m resolution DEMs used to measure erosional shorelines (Jewell, 2016), an important consideration when comparing the two studies. In addition, these depositional shorelines are not uniform in elevation and can vary 1 - 5 m along the crest of the feature. Though efforts were made to choose a central high point on the Bonneville, Provo, and intermediate barriers, the location of measurement could play a large role in the more variable relationship between Bonneville and Provo depositional shorelines.

Ground-Penetrating Radar

The GPR was unable to image deeper than 4 m in all of the profiles except one portion of the north-south profile at Horse Hills (Figure 4, Figure 5). A layer of fine-grained sediment covering the ground surface likely obstructed the EM radiation, making it difficult to penetrate to greater depth. The relatively shallow stratigraphy revealed by the GPR surveys provides some insight into the internal structure of these barriers but not enough to fully understand their construction.

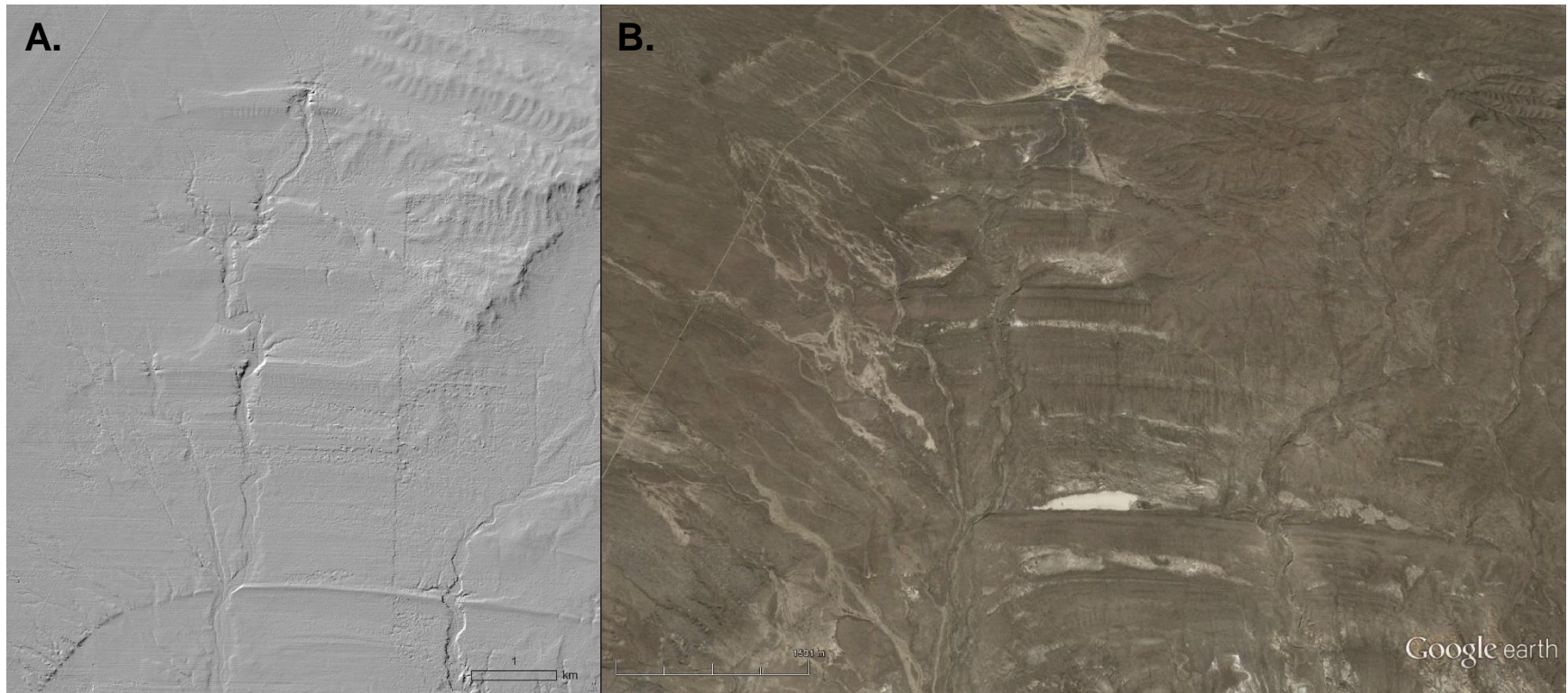


Figure 9. A stream drainage proves suitable conditions for the formation of barriers at Sevier 5 (Table 1). Modern streams cut through many of these deposits, leaving only small portions of the Pleistocene barriers in some places. Note the bright white marl deposits in the back lagoon of the Provo level barrier. A. 5-m DEM hillshade and B. GoogleEarth image.

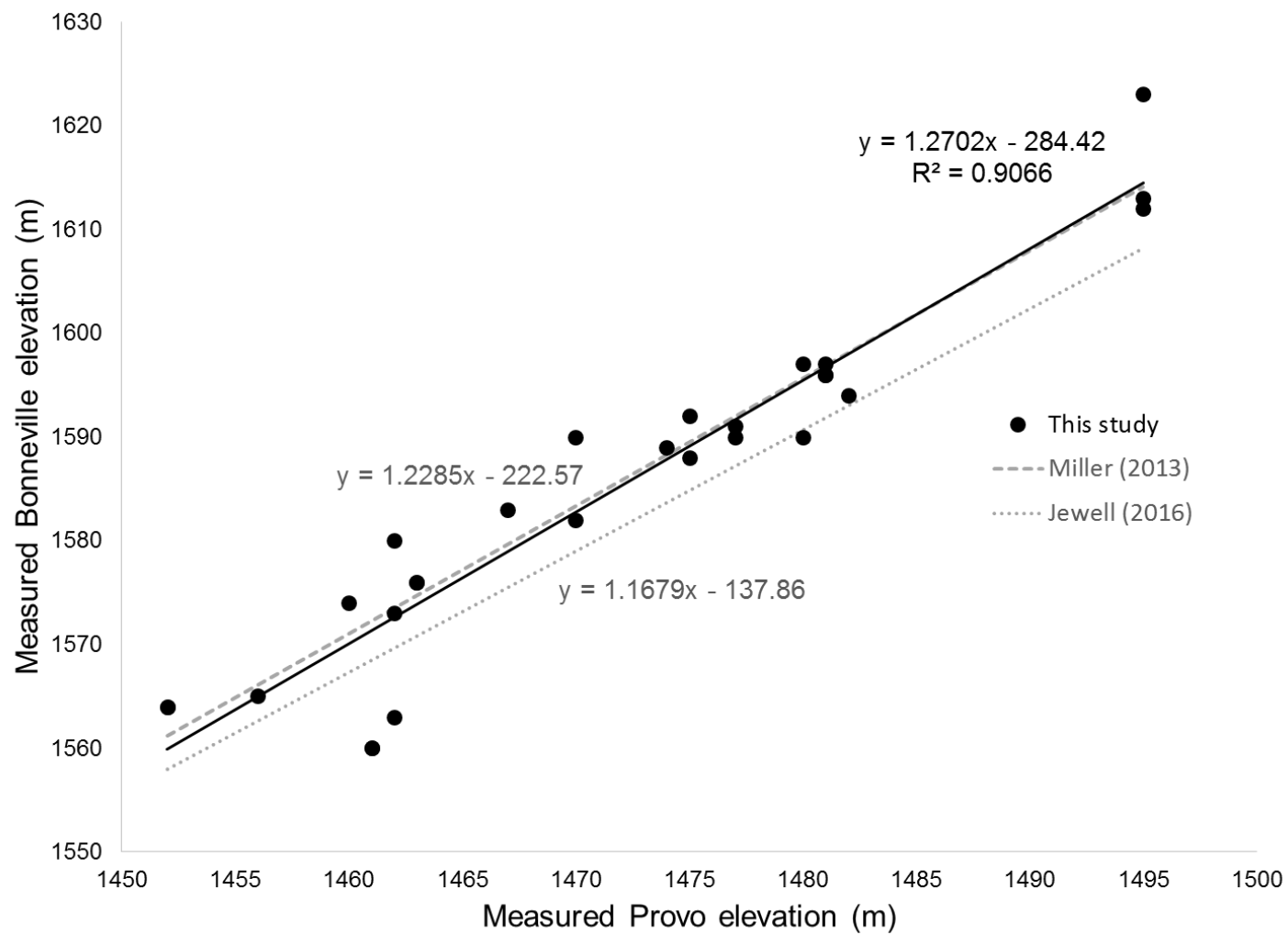


Figure 10. A scatterplot of measured Bonneville and upper Provo shoreline elevations.

The Bonneville-level barrier at Matlin 1 is characterized by lakeward sloping beds that are horizontal under the crest (Figure 4). On the back side (the mainland or lagoon side) of the barrier, beds are steeper and dip in the opposite direction. The surveyed barrier at the intermediate level is not as well defined, and GPR results indicate a buried shoreface infilled with horizontal beds on the lakeward-side of the structure. The shore-parallel transects from both barriers reveal relatively horizontal stratification with some undulations, possibly the result of surface disturbance during historic road construction or small break-through channels that formed during deposition.

At Horse Hills, a longer (120 m) cross-sectional profile shows clearer stratigraphy (Figure 5). Between 75 - 95 m on the north-south profile, the GPR resolved strata up to 8 m depth. On the south side, beds dip lakeward and steepen upward towards the ground surface. These beds appear to record lakeward aggradation as the crest of the barrier rose. The data are not as clear on the landward side of the feature - likely due to an increased amount of silt in the lagoon area - but the beds appear to slope at the same angle as the surface, reaching a horizontal orientation in the lagoon. The shore-parallel transect at Horse Hills is similar to transects at Matlin 1, with undulating subhorizontal beds.

Quantitative Analysis

Elevations of the crests of intermediate-level barriers were measured and plotted as a PDF using a 4-m moving window and 0.5-m interval (Figure 11). This is a larger spacing than was used by Jewell (2016) to identify erosional shorelines (3-m moving window and 0.25-m interval), but this spacing better accounts for the smaller sample size and greater vertical error inherited from the 5-m DEMs. Visual inspection of this

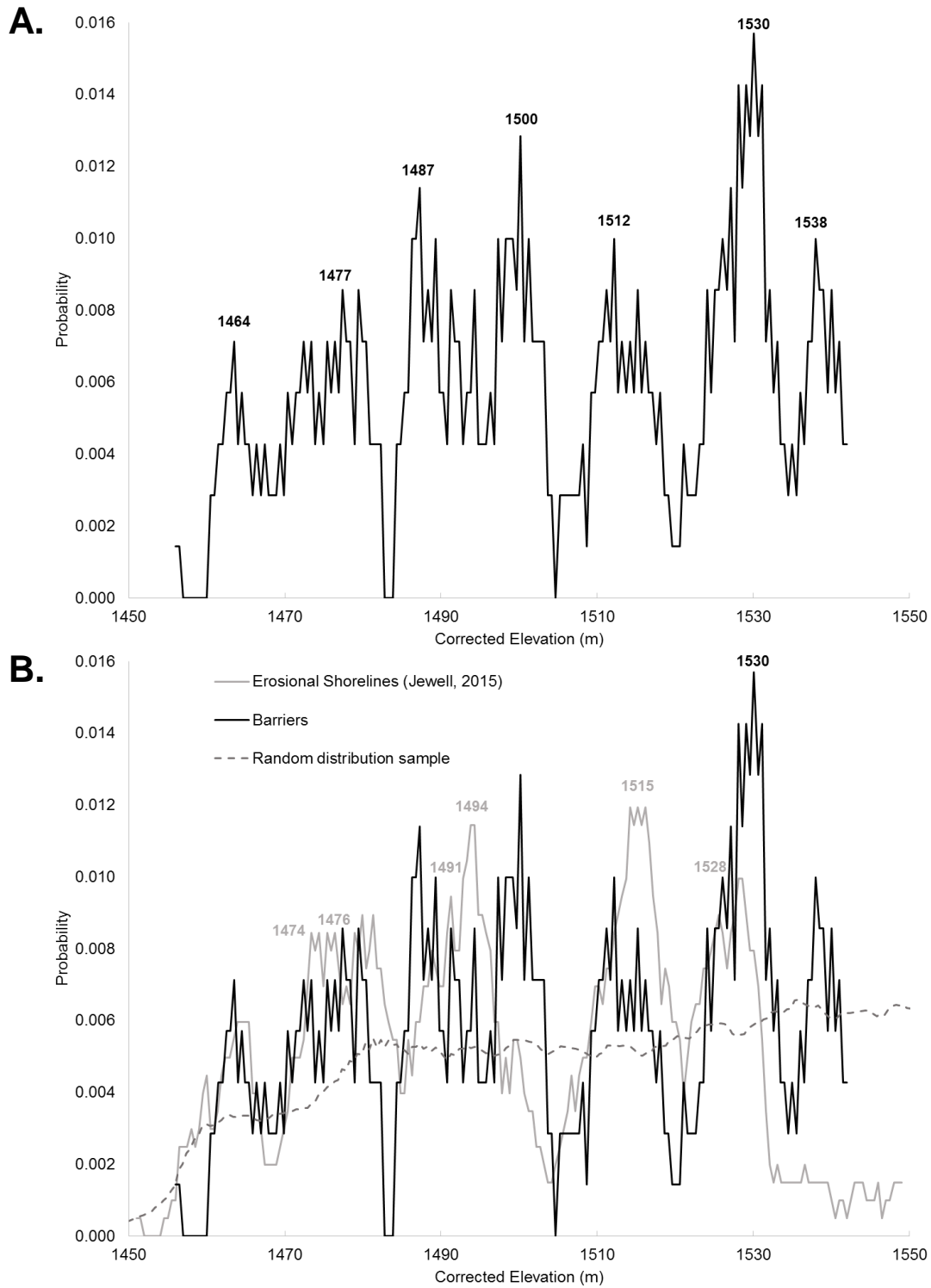


Figure 11. PDF plots evaluated with a 4-m moving window every 0.5 m. A. Intermediate barrier crest elevations corrected for isostatic rebound. Recorded elevations correspond to peaks identified through visual analysis. B. A comparison of this study to the measured elevations from Jewell (2016). The elevations of significant peaks are listed in colors that correspond to their data set. The random distribution sample was measured based on procedures outlined in Methods.

distribution of barrier elevations reveals one notable peak at 1530 m and a few smaller peaks at 1538 m, 1512 m, 1500 m, 1487 m, 1477 m, and 1464 m (Figure 11A). However, only the peak at 1530 m is determined to be significantly different from the random sampling of intermediate elevations. Furthermore, this elevation measurement has ± 4 m of error due to the 4-m moving window used to construct the PDF (Appendix B).

DISCUSSION

Controls on Barrier Bar Formation

Depositional features like barriers form when water level reaches a still-stand or proceeds to rise at a slow enough rate as to not over-top the landform. In theory, a lake rising at a constant rate with a constant rate of sediment supply would not leave behind any of these constructional landforms (Johnston, Thompson, & Baedke, 2007). Shoreline behaviors such as progradation, aggradation, and depositional transgression can only begin when there is an increase in the rate of water level change (Figure 12). When the rate of change reaches a certain threshold, determined by the relative availability of sediment, depositional transgression becomes the dominant shoreline process (Johnston et al., 2007). Likewise, the rate of sediment input also controls barrier construction. Gilbert (1885) noted that these features rely on shore drift for a continuous supply of new sediment but, when the sediment source is cut off, the waves that once worked to build the barrier will begin to excavate and destroy it. Thus, it is the rate of water level change, as well as changes in sediment availability, that ultimately determine the size and spacing of barrier systems (Johnston et al., 2007).

A common model for barrier response to rising water level includes three scenarios. The first is barrier erosion, in which the barrier profile moves upward at the same rate as water level rise. This model requires high rates of sediment supply and would place barrier development in the depositional regression and/or progradation realm

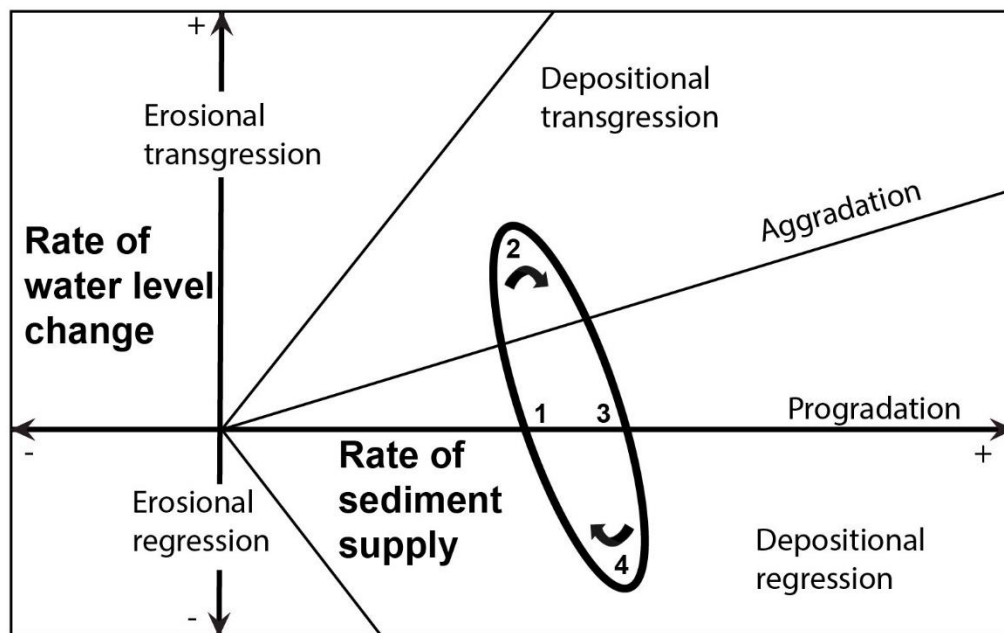


Figure 12. The relationship between changes in water level and sediment supply. A simplified cycle of barrier formation during an oscillation in water level is shown and numbered 1-4. After Johnson et al. (2007).

of Figure 12. The second is barrier translation, or the roll-over model, in which the barrier moves landward through shoreface erosion and subsequent deposition. In this case, the rate of water level change is greater than the rate of sediment supply and erosional and/or depositional transgression control barrier formation through washovers. The third scenario is barrier overstepping, which can only occur when the rate of water level rise outpaces the geomorphic response of the barrier. Barrier overstepping is not common in marine settings but may be more prevalent in a closed basin lake where shore zones are steeper and water level oscillates on shorter time scales (Masselink & Hughs, 2003). It is difficult to determine the role of barrier erosion and translation in the formation and movement of features mapped in this study with the constraints of relatively shallow GPR surveys. Better exposures of the internal structure of intermediate barriers would help further our understanding of their geomorphic history.

Due to local variations in measured elevation and morphology, the formation of barriers in Lake Bonneville appears to be controlled by more than relative water level alone. The availability of a sediment source, fetch at a given location, and geomorphic protection determine the likelihood that these features will form and be preserved over time. As the lake transgressed, waves met new sediment sources at different locations and elevations, which could then be used to construct depositional landforms. This positioning of available sediment likely played a large role in determining the spacing between individual barriers.

The wave energy required to move sediment may also be an important consideration in understanding the formation of barriers. Locations with large fetch and relatively high wave energy may be too energetic to leave behind constructional features,

easily depleting the sediment source and instead eroding cut-terraces and sea cliffs. Furthermore, in areas with slack water and little wave energy, waves may not be able to move enough sediment to build such large shore deposits. Most of the barriers investigated in this study are found in coves, bays, and other moderately protected areas with a small bedrock ridge on at least one side. This type of shore morphology likely encourages longshore drift and the appropriate wave energy for building and preserving barriers, while also providing an additional sediment source. These findings are consistent with Gilbert's (1885; 1890, p. 123) hypotheses that the elevations of depositional features depend on complex local conditions, as well as with previous studies of local variation in lacustrine shoreline elevations (Adams & Wesnousky, 1998; Atwood, 1994).

The Dugway barrier system provides an interesting example of extremely local variations in shoreline morphology. At this location, barriers appear at first glance to have been formed at the same water level, but they differ by up to 50 m in elevation (Figure 8). The variations in barrier height are likely caused by responses to the availability of sediment, longshore drift, and the slope of the shore zone. The eastern barriers accumulated sediment from the adjacent alluvial fan, as longshore currents deposited the sediment against the eastern side of the bedrock ridge. Barriers found to the west of this ridge do not have direct access to such a large sediment source or unobstructed longshore currents, and consequently cannot reach the same heights as those to the east. Although the barriers on either side of the bedrock ridge appear to form a linear shoreline, it cannot be determined whether they formed while the lake was at the same level. On one hand, the eastern barriers have an abundant sediment supply paired

with a significantly longer fetch, capable of producing powerful waves, especially during storms. On the other hand, 50 m of accumulation may be more than can be explained by waves and sediment supply alone. The western shore has a shallower slope than the eastern shore, and it may only be coincidence that these three barriers align.

Interpreting the Subsurface

GPR profiles from Horse Hills and Matlin 1 are consistent with observations by Adams and Wesnousky (1998) describing the stratigraphy of barriers in paleolake Lahontan. In both locations, the interior geometry of the barrier closely mimics their convex-up form. Adams and Wesnousky (1998) found this morphology and their more extensive exposure of subsurface stratigraphy to be indicative of barrier rollover (translation). Assuming the interiors of Lake Bonneville barriers match those studied in Lake Lahontan, it can be inferred that these constructional features underwent the same type of landward migration. As large storm waves passed over the barriers, they eroded sediment from the shoreface and deposited it on the leeward side, thus forming the convex-up stratigraphy (Masselink & Hughs, 2003).

Significance of Barrier Elevations and Comparison to Erosional Shorelines

Using the statistical methods outlined above, only one intermediate barrier elevation, 1530 \pm 4 m, was found to be statistically significant. Although visual analysis of Figure 11A may indicate up to six other intermediate levels (1538, 1512, 1500, 1487, 1477, 1464), these peaks cannot be confidently distinguished from the random sampling of intermediate elevations (Appendix B). However, this does not mean that these peaks

do not represent a real correlation, only that there are not enough measurements to determine basin-wide shoreline elevations with confidence.

When the same statistical methods were applied to the erosional shorelines of Jewell (2016), the following six elevations were found to be significant: 1528 m, 1515 m, 1494 m, 1491 m, 1476 m, and 1474 m (Figure 11). Again, these elevations have ± 4 m error due to the size of the moving window. Jewell (2016) likely had more success correlating intermediate shorelines due to the availability of higher resolution DEMs and the increased number of erosional cut terraces in the sample he used. Barriers are not nearly as widespread as erosional shorelines, limiting this study to shore zones capable of supporting barrier formation and preservation. Even within these limitations, there is still a noticeable correlation between the 1530 m and 1528 m levels measured from barriers and erosional shorelines, respectively (Figure 11B). The two peaks in each data set indicate a correlatable intermediate shoreline, present in both erosional and depositional features. Gilbert (1890) noted that, although cut terraces and sea cliffs offer a more reliable record of persistent water levels, the presence of coordinated erosional and depositional features provides “an additional mark of persistent stages” (p. 146). Thus, the corresponding elevations found in both records further confirm the presence of a basin-wide intermediate level at about an adjusted altitude of 1530 m.

Despite this strong correlation, it is important to note that these elevations do not represent the water’s edge, but are rather a datum for relating common shorelines. The elevations measured in this study and Jewell (2016) more likely represent the elevation of breaking waves during the largest storm events. Most geomorphic work is accomplished in these large, infrequent events, capable of moving and eroding exponentially more

material than persistent waves and currents (Gilbert, 1885).

Paleoclimate Implications

Understanding the timing and nature of lake level changes during the late Pleistocene can provide insight into the paleoclimate of the interior western United States. Oviatt (1997) used radiocarbon dating from deep-water cores and from gravel wedges in shorezone settings to outline three falling-lake events (U1, U2, U3) that occurred during transgressive-phase Lake Bonneville. Using the limited radiocarbon data available at the time, Oviatt (1997) thought that each of these falling-lake events is synchronous with the ends of iceberg-rafting events in the North Atlantic Ocean, suggesting a link between Great Basin hydroclimate and changes in the Northern Hemisphere ice sheets. The occurrence of these falling-lake events confirms that the lake's transgression was oscillatory and not a continuous rise marked by intermittent still-stands. A further complication in understanding the ages of intermediate barrier systems is that precise ages have not been determined. The assumption that they decrease in age linearly with elevation makes sense in the context of the available radiocarbon ages from the basin (Figure 2).

Despite uncertainties in numerical age, the spacing between barriers provides some indication about the nature of water level changes. Barrier overstepping occurs when the rate of water level rise outpaces the geomorphic response of the barrier. Thus, in order to construct individual barriers, the lake would need to rise fast enough to overstep a barrier without significantly eroding its form. The relatively broad, flat tops of the intermediate barriers, compared to the sharper, narrower form of those at the

Bonneville level, are likely the result of water level change slowing to a halt at the tops of oscillation events (Figure 3, Figure 8). The Bonneville shoreline was quickly abandoned during the Bonneville flood and therefore does not record the same history of water level change. The presence and morphology of these forms supports the hypothesis that transgressive-phase Lake Bonneville was marked by multiple, rapid changes in water level, some of which are shown to correspond with larger scale climate events. Further investigation of the ages of these barriers may provide a unique climate record for the interior western United States during the late Pleistocene.

CONCLUSIONS

1. The barrier systems in late Pleistocene Lake Bonneville provide one confidently correlatable intermediate depositional shoreline at an isostatically adjusted elevation of 1530 \pm 4 m. This elevation also corresponds with the 1528 m shoreline determined by a survey of erosional shorelines (Jewell, 2016), offering more evidence of this basin-scale intermediate shoreline.
2. Potential error in corrections for isostatic rebound, as well as the vertical resolution of the DEMs used in this study, complicate the likelihood of clearly identifying multiple intermediate shorelines. In addition, previous studies of lacustrine shorelines demonstrate that lake levels and depositional features can vary up to two or three meters in elevation in relatively small geographic areas (Adams & Wesnousky, 1998; Atwood, 1994).
3. Lake Bonneville barriers display a wide range of morphologies determined by local sediment supply, wave energy, and other geomorphic conditions. The formation of these barriers cannot be described with one single theory since local factors have greater control on their elevations, shapes, and positions than basin-scale water level changes.
4. The subsurface stratigraphy of surveyed barriers reveals landward migration through barrier rollover during periods of relatively stable lake levels and/or periods of gradual water level rise.

5. The spacing of barriers indicates multiple, relatively fast changes in lake level during the late Pleistocene. Previous studies have linked transgressive-stage oscillations to global climate events and further studies of Lake Bonneville's intermediate shorelines could provide a unique record of interior terrestrial climate and its connection to global-scale events.

APPENDIX A

DETAILED RESULTS OF GROUND-PENETRATING RADAR

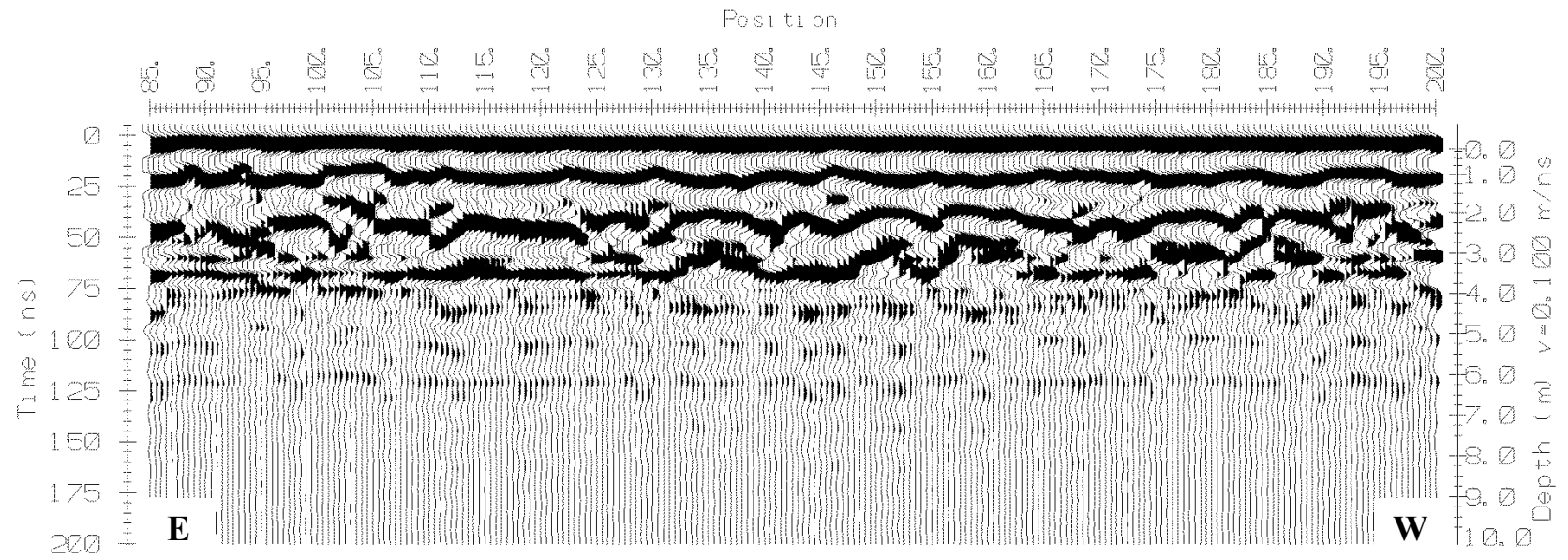


Figure 13. GPR survey at Matlin 1 on the Bonneville-level barrier. East (12N 304939 4609877) to west (12N 304731 4609873). Position on the horizontal axis is given in meters.

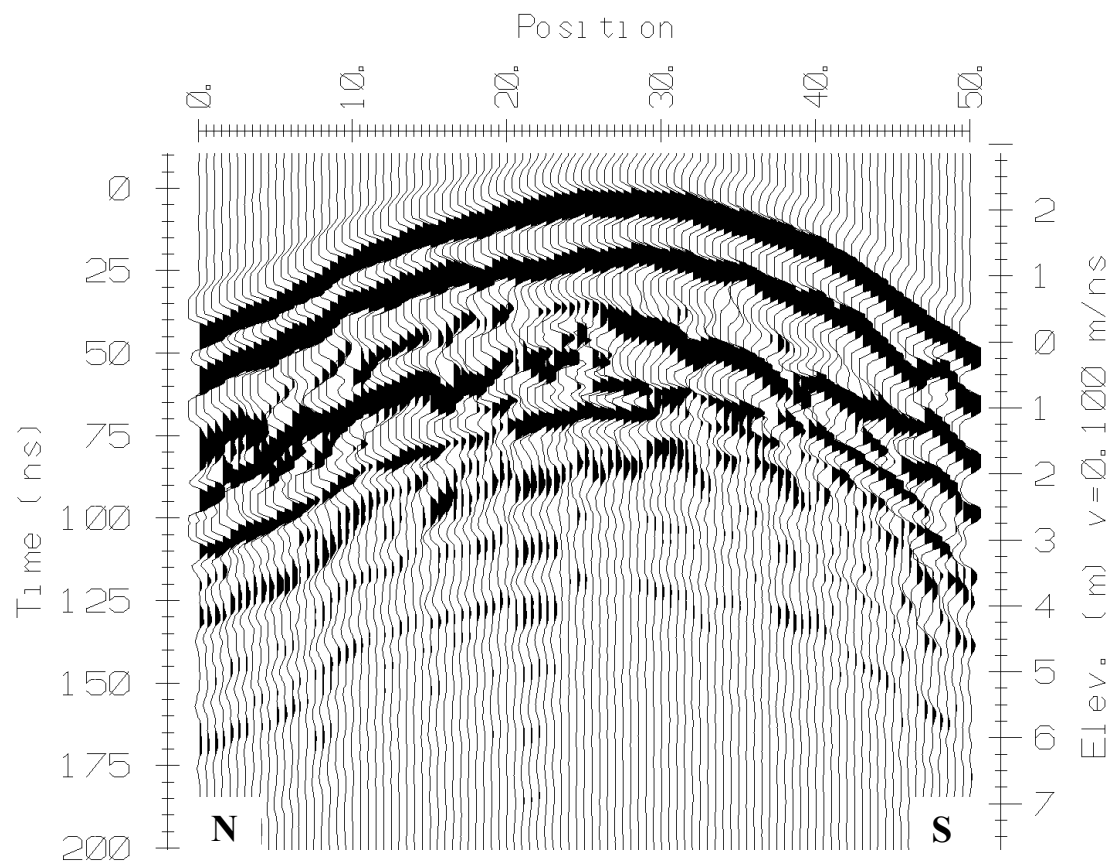


Figure 14. GPR survey at Matlin 1 on the Bonneville-level barrier. North (12N 304829 4609910) to south (12N 304832 4609862).

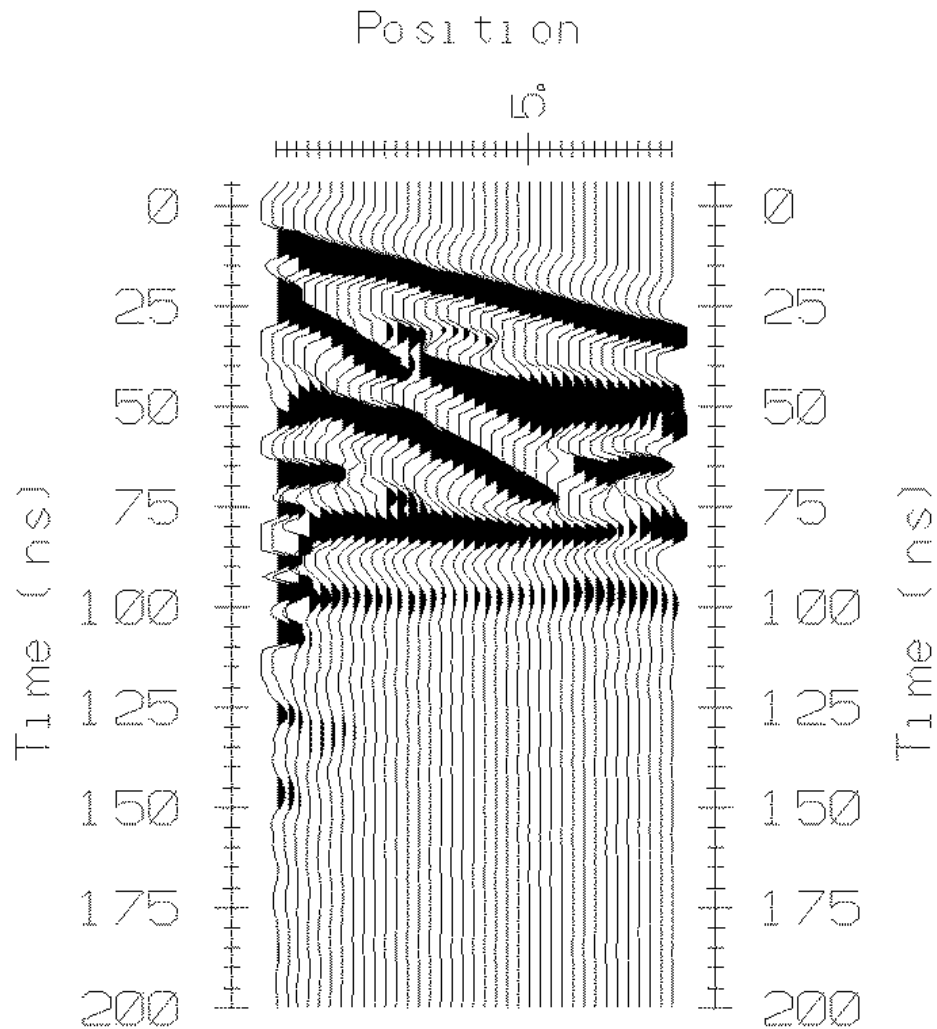


Figure 15. A common midpoint sounding at Matlin 1. This survey was taken on the Bonneville-level barrier and uses the inverse slope of the ground wave to determine the propagation velocity of electromagnetic wave energy of the sediment. This allows the measured two way travel time to be transformed to depth without invasive methods. The calculated velocity for all profiles surveyed in this study is 0.1 m/ns.

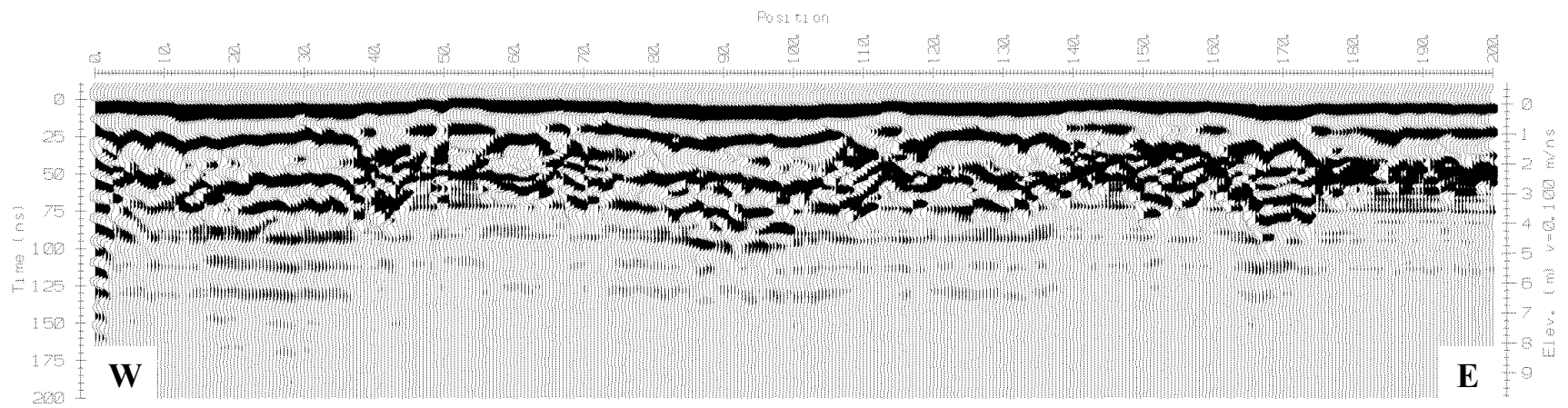


Figure 16. GPR survey at Matlin 1 on an intermediate-level barrier. West (12N 305305 4607477) to east (12N 305502 4607436).

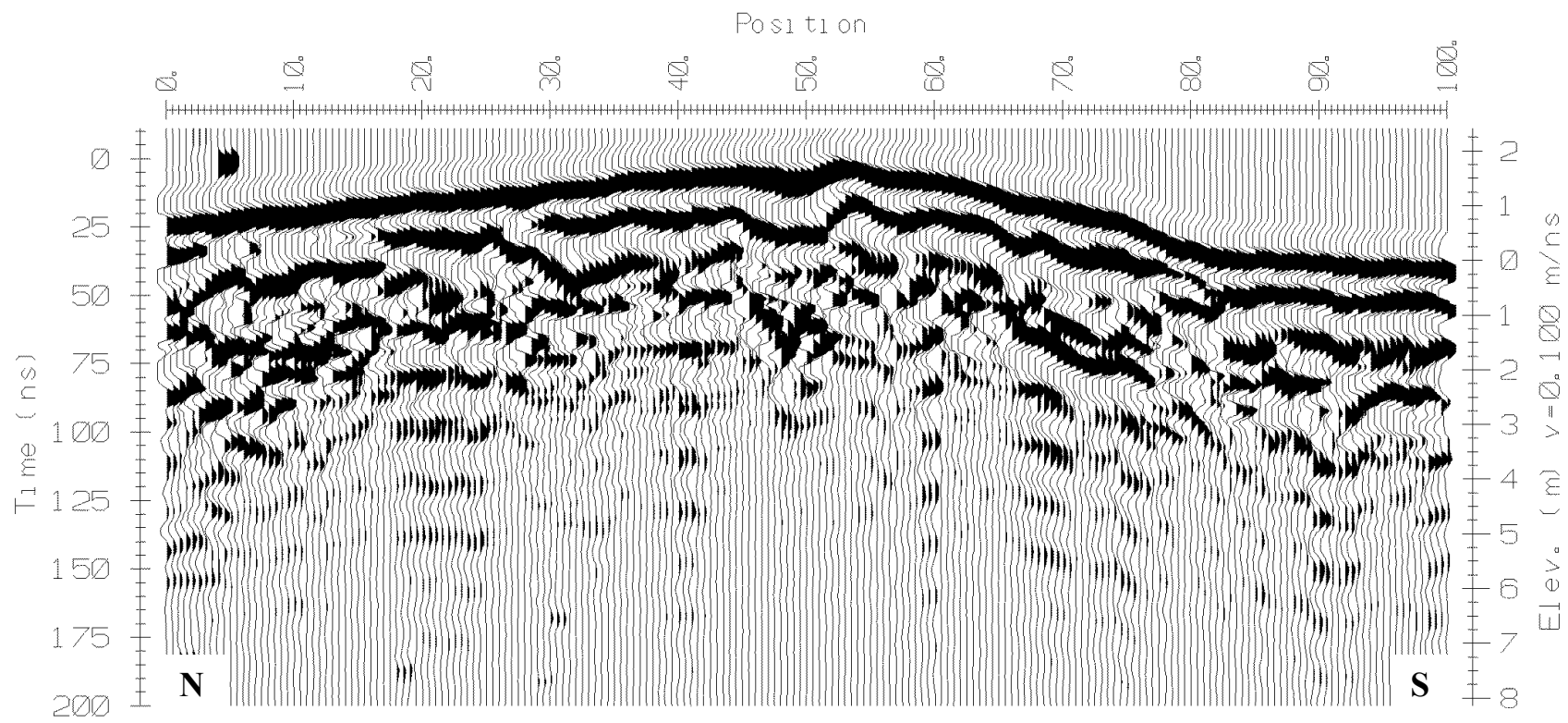


Figure 17. GPR survey at Matlin 1 on an intermediate-level barrier. North (12N 305418 4607500) to south (12N 305392 4607404).

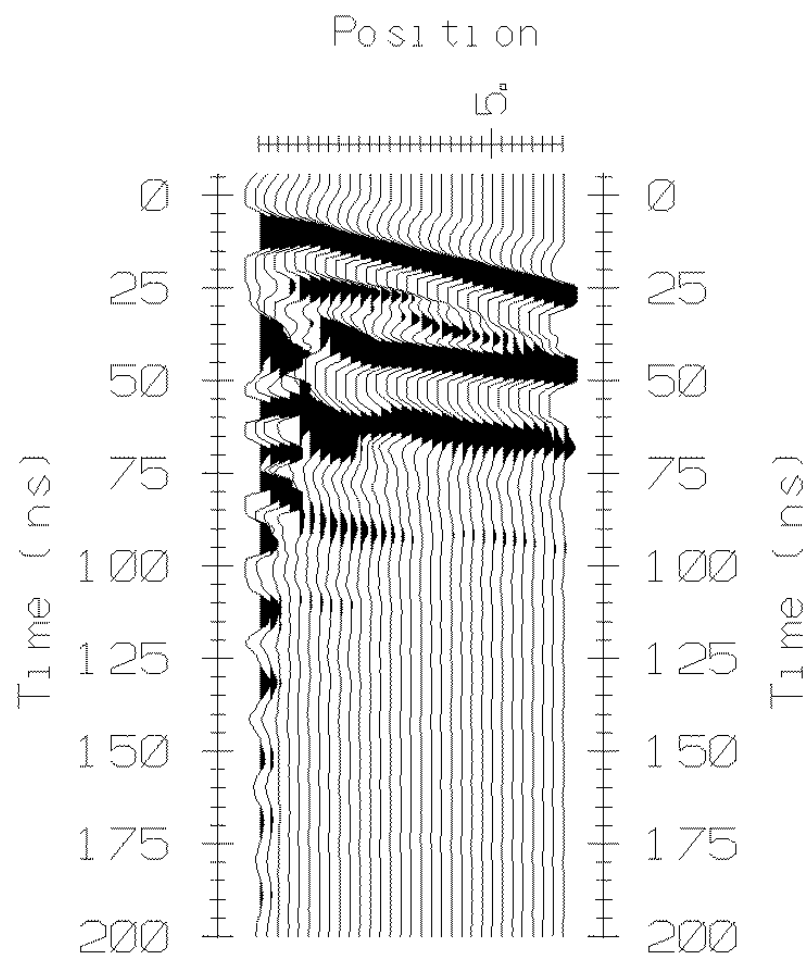


Figure 18. A common midpoint sounding at Matlin 1. This survey was taken on the intermediate-level barrier and reveals a propagation velocity of 0.1 m/ns.

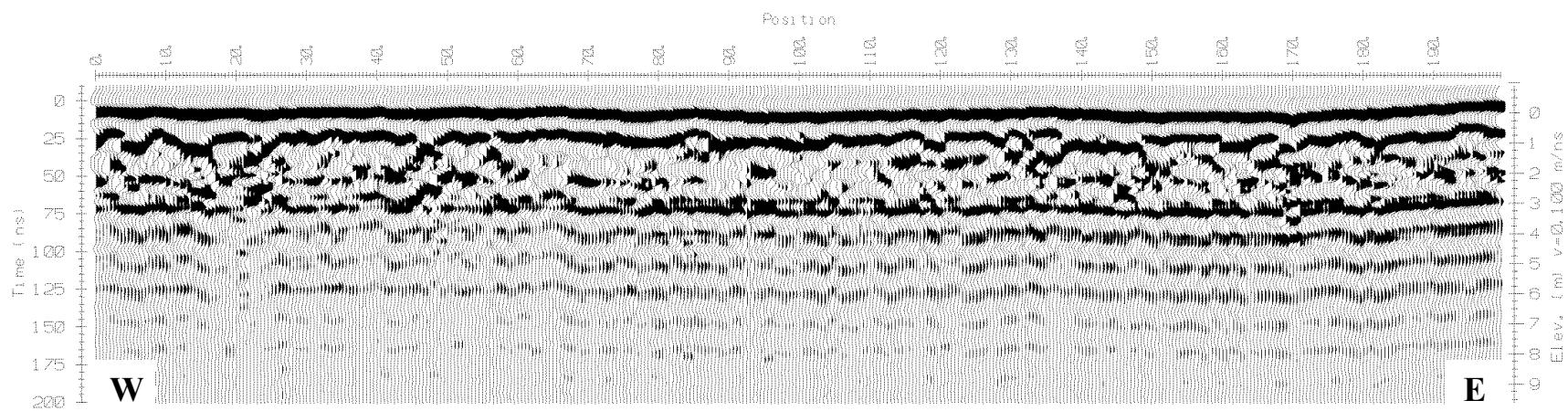


Figure 19. GPR survey at Horse Hills 2 on the Bonneville-level barrier. West (12N 297384 4611494) to east (12N 297575 4611436).

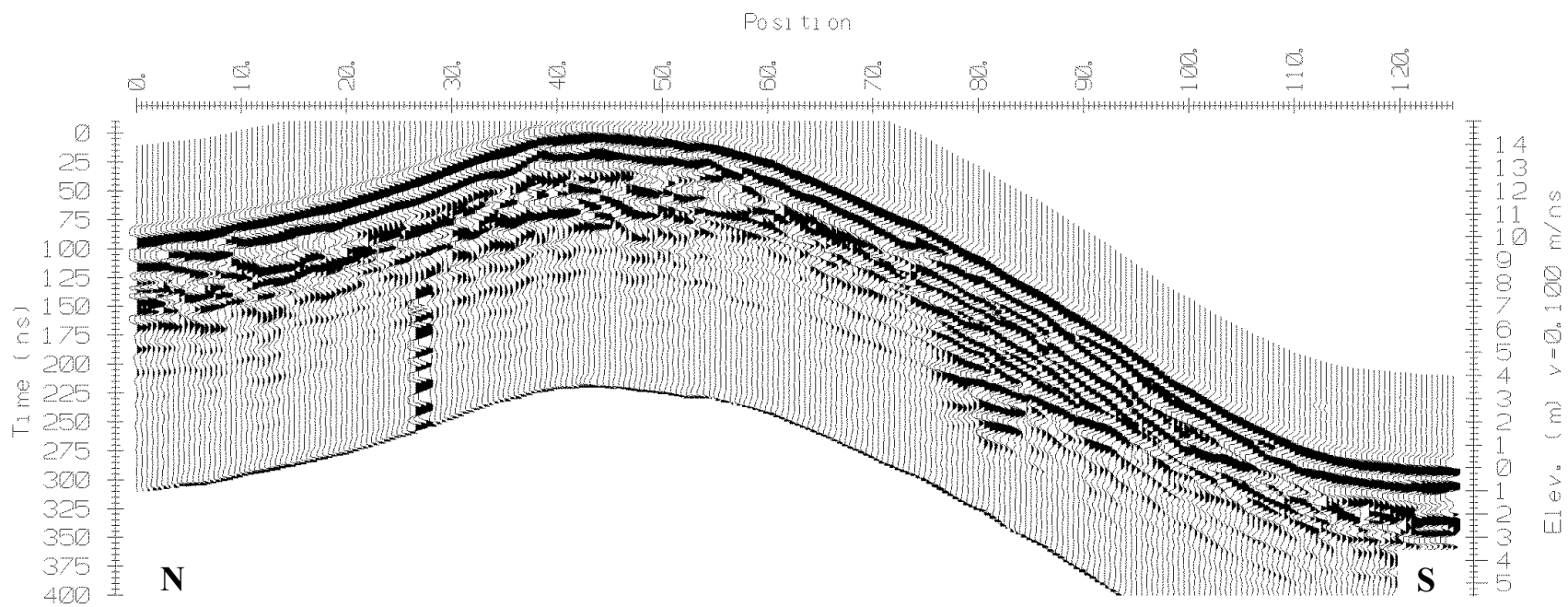


Figure 20. GPR survey at Horse Hills 2 on the Bonneville-level barrier. North (12 N 297494 4611514) to south (12 N 297455 4611384).

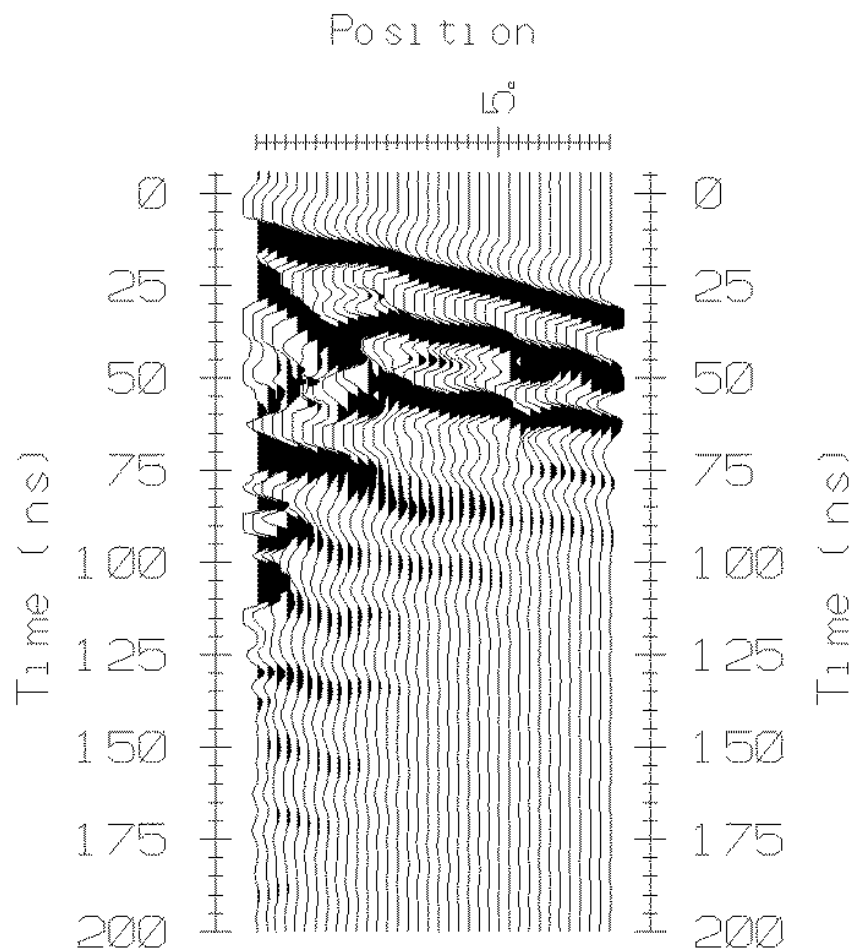


Figure 21. A common midpoint sounding at Horse Hills 2. This survey was taken on the Bonneville-level barrier and reveals a propagation velocity of 0.1 m/ns.

APPENDIX B

QUANTITATIVE ANALYSES

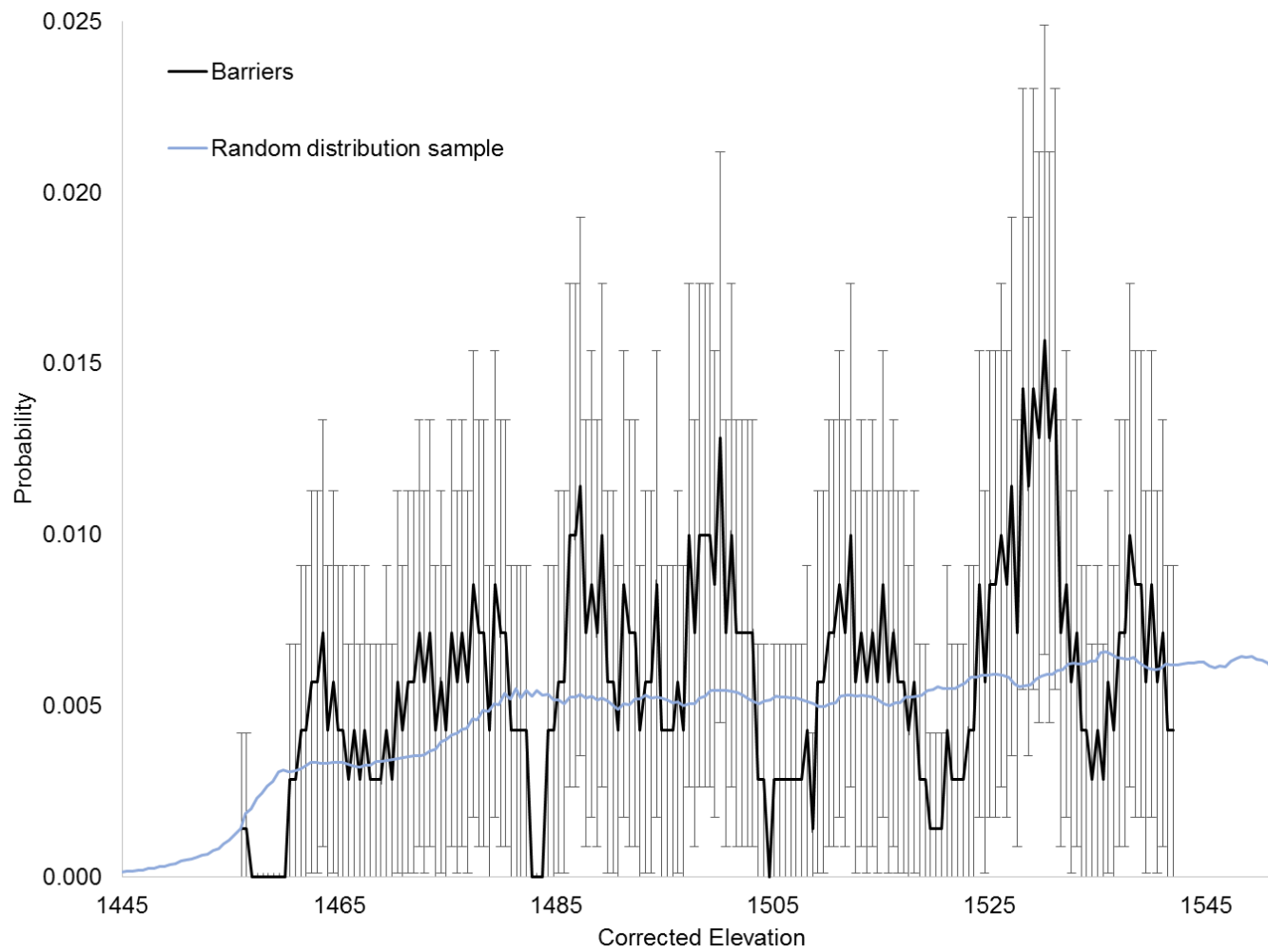


Figure 22. PDF plot of barrier and random sample elevations. 4 m moving window and 0.5 m spacing with error bars determined using Eq. 4.

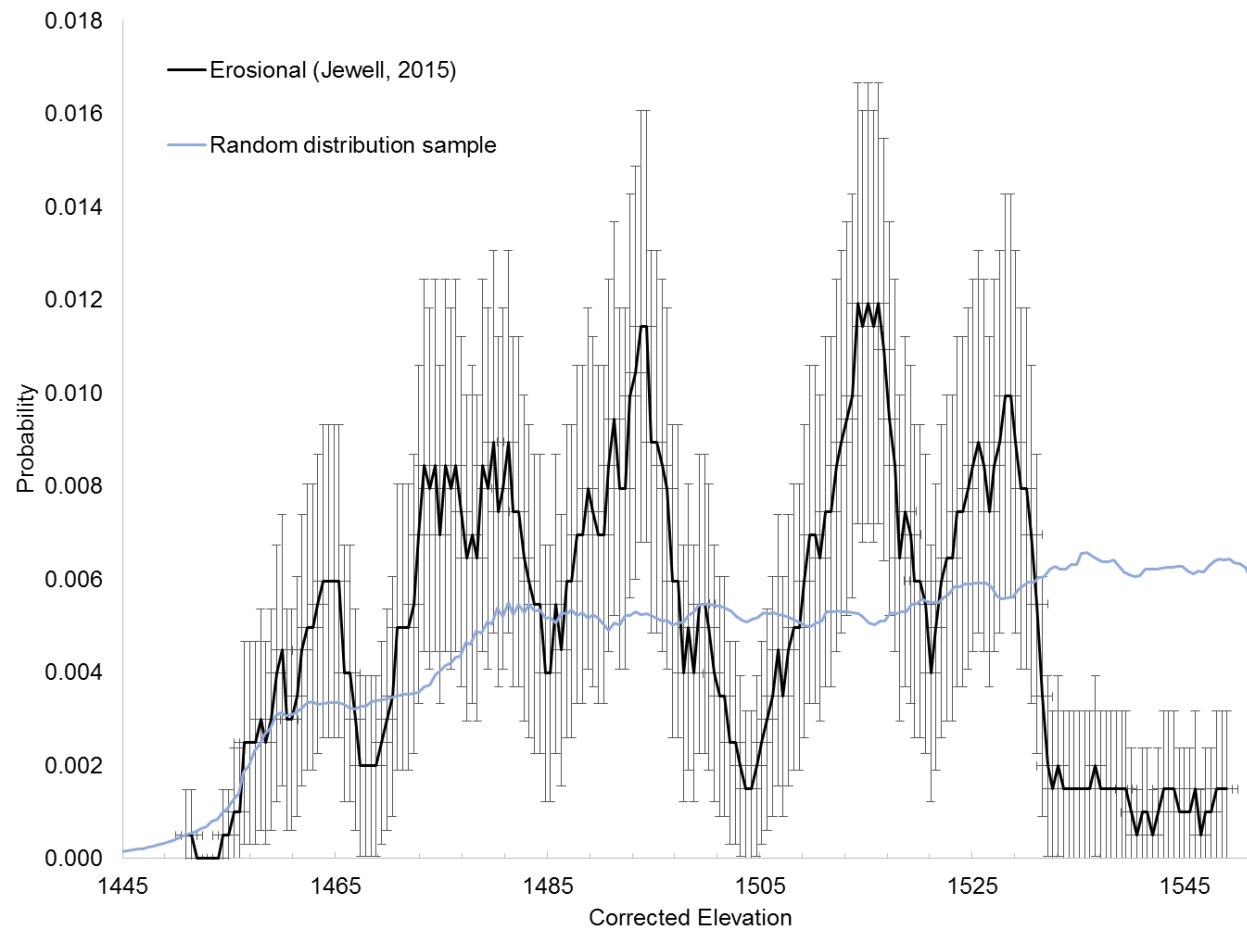


Figure 23. PDF plot of erosional shorelines and random sample elevations. 4 m moving window and 0.5 m spacing with error bars determined using Eq. 4.

REFERENCES

- Adams, K. D., & Wesnousky, S. G. (1998). Shoreline processes and the age of the Lake Lahontan highstand in the Jessup embayment, Nevada. *Bulletin of the Geological Society of America*, 110(10), 1318–1332.
- Atwood, G. (1994). Geomorphology applied to flooding problems of closed-basin lakes, specifically Great Salt Lake, Utah. *Geomorphology*, 10, 197.
- Benson, L. V., Currey, D. R., Dorn, R. I., Lajoie, K. R., Oviatt, C. G., Robinson, S. W., & Stine, S. (1990). Chronology of expansion and contraction of four Great Basin lake systems during the past 35,000 years. *Palaeogeography, Palaeoclimatology, Palaeoecology*, 78, 241–286.
- Bird, E. (2008). *Coastal geomorphology*. Chichester, UK: Wiley.
- Cressie, N. A. C., & Wikle, C. K. (2011). *Statistics for spatio-temporal data*. Hoboken, NJ: Wiley.
- Currey, D. R. (1982). Lake Bonneville: Selected features of relevance to neotectonic analysis. *U.S. Geological Survey Open-File Report*, 82-1070, 1–30.
- Currey, D. R. (1990). Quaternary paleolakes in the evolution of semidesert basins, with special emphasis on Lake Bonneville and the Great Basin, U.S.A. *Palaeogeography, Palaeoclimatology, Palaeoecology*, 76(3-4), 189–214.
- Currey, D. R., & Oviatt, C. G. (1985). Durations, Average Rates, and Probable Causes of Lake Bonneville Expansions, Stillstands, and Contractions During the Last Deep-Lake Cycle, 32,000 to 10,000 Years Ago. *Problems of and Prospects for Predicting Great Salt Lake Levels - Papers from a Conference Held in Salt Lake City*.
- Davis, R. A. (1994a). Barrier island systems - a geologic overview. In R. A. Davis (Ed.), *Geology of Holocene barrier island systems* (pp. 1–46). Berlin: Springer-Verlag.
- Gilbert, G. K. (1890). Lake Bonneville. *US Geological Survey Monograph 1*, 438.
- Gilbert, G. K. (1885). The topographic features of lake shores. *USGS Annual Report 5-B*, 88–96.

- Godsey, H. S., Currey, D. R., & Chan, M. a. (2005). New evidence for an extended occupation of the Provo shoreline and implications for regional climate change, Pleistocene Lake Bonneville, Utah, USA. *Quaternary Research*, 63(2), 212–223.
- Godsey, H. S., Oviatt, C. G., Miller, D. M., & Chan, M. a. (2011). Stratigraphy and chronology of offshore to nearshore deposits associated with the Provo shoreline, Pleistocene Lake Bonneville, Utah. *Palaeogeography, Palaeoclimatology, Palaeoecology*, 310(3-4), 442–450.
- Hesp, P. A., & Short, A. D. (1999). Barrier morphodynamics. In A. D. Short (Ed.), *Handbook of beach and shoreface morphodynamics* (pp. 307–333). New York, NY: Wiley.
- Janecke, S., & Oaks, R. (2011). New insights into the outlet conditions of late Pleistocene Lake Bonneville, southeastern Idaho, USA. *Geosphere*, 7(6), 1369.
- Jewell, P. W. (2016). Quantitative identification of erosional Lake Bonneville shorelines, Utah. *Geomorphology*, 253, 135–145.
- Johnston, J. W., Thompson, T. A., & Baedke, S. J. (2007). Systematic pattern of beach-ridge development and preservation: Conceptual model and evidence from ground penetrating radar. *Special Paper - Geological Society of America*, 432, 47–58.
- Jol, H. M., & Bristow, C. S. (2003). GPR in sediments: Advice on data collection, basic processing and interpretation, a good practice guide. *Geological Society, London, Special Publications*, 211, 9–27.
- Leatherman, S. P. (1988). *Barrier island handbook* (3rd ed.). College Park, MD: Coastal Publications Series, Laboratory for Coastal Research, The University of Maryland.
- Miller, D. M., Oviatt, C. G., & Mcgeehin, J. P. (2013). Stratigraphy and chronology of Provo shoreline deposits and lake-level implications, Late Pleistocene Lake Bonneville, eastern Great Basin, USA. *Boreas*, 42(2), 342–361.
- Oviatt, C. G. (1997). Lake Bonneville fluctuations and global climate change. *Geology*, 25(2), 155–158.
- Oviatt, C. G. (2015). Chronology of Lake Bonneville, 30,000 to 10,000 yr B.P. *Quaternary Science Reviews*, 110, 166–171.
- Oviatt, C. G., Currey, D. R., & Sack, D. (1992). Radiocarbon chronology of Lake Bonneville, Eastern Great Basin, USA. *Palaeogeography, Palaeoclimatology, Palaeoecology*, 99, 225–241.
- Woodroffe, C. D. (2003). *Coasts: form, process, evolution*. Cambridge, UK: Cambridge University Press.